Cerebral Cortex November 2010;20:2712–2727
doi:10.1093/cercor/bhq017
Advance Access publication March 1, 2010

Improved Reversal Learning and Working Memory and Enhanced Reactivity to Novelty in Mice with Enhanced GABAergic Innervation in the Dentate Gyrus

Fabio Morellini[1,2], Elena Sivukhina[1], Luminita Stoenica[1,3], Elena Oulianova[1], Olena Bukalo[1], Igor Jakovcevski[1], Alexander Dityatev[1,3,4], Andrey Irintchev[1,5] and Melitta Schachner[1,6,7]

[1]Zentrum für Molekulare Neurobiologie Hamburg, Universitätsklinikum Hamburg-Eppendorf, 20246 Hamburg, Germany, [2]Experimentelle Neuropädiatrie, Universitätsklinikum Hamburg-Eppendorf, 20246 Hamburg, Germany, [3]Institut für Neurophysiologie und Pathophysiologie, Universitätsklinikum Hamburg-Eppendorf, 20246 Hamburg, Germany, [4]Department of Neuroscience and Brain Technologies, Italian Institute of Technology, 16163 Genova, Italy, [5]Department of Otorhinolaryngology, Friedrich Schiller University Jena, 07740 Jena, Germany, [6]Department of Cell Biology and Neuroscience, Keck Center for Collaborative Neuroscience, Rutgers University, Piscataway, NJ 08854, USA and [7]Center for Neuroscience, Shantou University Medical College, Shantou 515041, China

Fabio Morellini, Elena Sivukhina, and Luminita Stoenica contributed equally to this work.

Address correspondence to Fabio Morellini, Experimentelle Neuropaediatrie, Universitaetsklinikum Hamburg-Eppendorf, Martinistrasse 52, 20246 Hamburg, Germany. Email: fabio.morellini@enp.org.

The balance between excitation and inhibition controls fundamental aspects of the hippocampal function. Here, we report an increase in the ratio of inhibitory to excitatory neurons in the dentate gyrus, accompanied by γ-aminobutyric acid$_A$ (GABA$_A$) receptor–dependent impairment of synaptic plasticity and enhancement of activity-dependent changes in excitability in anesthetized adult mice deficient for the extracellular matrix glycoprotein tenascin-R (TNR). TNR-deficient mice showed faster reversal learning, improved working memory, and enhanced reactivity to novelty than wild-type littermates. Remarkably, in wild-type and TNR-deficient mice, faster reversal learning rates correlated at the individual animal level with ratios of parvalbumin-positive interneurons to granule cells and densities of parvalbumin-positive terminals on somata of granule cells. Our data demonstrate that modification of the extracellular matrix by ablation of TNR leads to a new structural and functional design of the dentate gyrus, with enhanced GABAergic innervation, that is, enhanced ratio of inhibitory to excitatory cells, and altered plasticity, promoting working memory and reversal learning. In wild-type mice, the enhanced ratio of inhibitory to excitatory cells in the dentate gyrus also positively correlated with reversal learning, indicating that level of inhibition regulates specific aspects of learning independent of the TNR gene.

Keywords: behavior, electrophysiology, hippocampus, inhibition, morphology

Introduction

Functional circuits in the central nervous system (CNS) depend on a finely tuned balance between synaptic excitation and inhibition and disruption of this balance in the cortex can lead to cognitive disorders and schizophrenia in humans (Lewis et al. 2005; Woo and Lu 2006). It is accepted that specific forms of synaptic plasticity such as long-term potentiation (LTP) in the hippocampus are mediated by excitatory principal neurons under the control of several classes of inhibitory interneurons (Cobb et al. 1995; Freund and Buzsáki 1996; McBain and Fisahn 2001; Mitchell and Silver 2003). In particular the dentate gyrus, which receives sensory information via the perforant path fibers, is characterized by low levels of excitability and by a unique and complex assortment of γ-aminobutyric acid$_A$ (GABA$_A$) receptor subunits expressed by its granule cells (Barnard et al. 1998; Wei et al. 2003).

This study addressed the question of how an alteration in the number of inhibitory interneurons in the dentate gyrus affects the GABAergic projections to principal cells and, as a consequence, synaptic plasticity in vivo and cognitive functions of mice. As a model, we used mice deficient in the extracellular glycoprotein tenascin-R (TNR) (Weber et al. 1999). TNR is expressed in the CNS of vertebrates and synthesized by Purkinje cells, motoneurons, subpopulations of interneurons, and oligodendrocytes (Fuss et al. 1993; Wintergerst et al. 1993; Woodworth et al. 2002). In contrast to oligodendrocytes, TNR expression in neurons does not decrease in the adult and concentrates in perineuronal nets surrounding fast-spiking parvalbumin-positive (PV$^+$) interneurons (Härtig et al. 1992; Wintergerst et al. 1993; Berghuis et al. 2004) that are of crucial importance for shaping synchronized activity of neuronal ensembles (Freund 2003).

Here, we report that TNR deficiency leads to an increase in the number of PV$^+$ interneurons and principal cells in the hippocampus. In the dentate gyrus, but not in the other hippocampal subfields, the ratio of PV$^+$ interneurons to granule cells and number of GABAergic terminals on somata of granule cells are strongly increased. These structural aberrations correlate with alterations in GABA$_A$ receptor–dependent neuronal plasticity in the dentate gyrus and faster reversal learning and enhanced working memory of TNR-deficient mice.

Materials and Methods

Animals

TNR-deficient (TNR−/−) and wild-type (TNR+/+) male littermates with a C57BL/6J genetic background after 5 backcrosses of mice from the original C57BL/6J × 129/Ola colony (Weber et al. 1999) were used. The animals were bred at the pathogen-free animal facility of the University of Hamburg. Behavioral experiments were performed on separate batches of 3- to 5-month-old male mice. Morphological investigations were performed on 5-month-old animals that had been used in the water-maze test. For electrophysiological recording of dentate gyrus LTP, 4-month-old male mice were used. In addition to adult animals, 7-day-old mice were used for morphological assessment of cell proliferation and apoptosis. Experiments were conducted in accordance with the German and European Community laws on protection of experimental animals and approved by the local authorities of the City of Hamburg.

Morphological Analysis

Preparation of Tissue Samples and Immunohistochemistry

Tissue preparation and immunohistochemical stainings were performed as described (Irintchev et al. 2005). Mice were anesthetized with sodium pentobarbital (Narcoren, Merial, Hallbermoos, Germany, 5 μL/g body weight, i.p.) and perfused transcardially with saline (0.9% NaCl) followed by fixative (4% formaldehyde and 0.1% $CaCl_2$ in 0.1 M cacodylate buffer, pH 7.3, 15 min at room temperature, RT). The brains were postfixed overnight at 4 °C in the fixative solution supplemented with 15% sucrose, followed by immersion in 15% sucrose solution in 0.1 M cacodylate buffer, pH 7.3, for an additional day at 4 °C. The tissue was frozen for 2 min in 2-methyl-butane (isopentane) precooled to −30 °C in the cryostat (Leica CM3050, Leica Instruments, Nußloch, Germany) and stored in liquid nitrogen until sectioned. Serial coronal sections of 25-μm thickness were cut in a caudal-to-rostral direction and collected on SuperFrostPlus glass slides (Roth, Karlsruhe, Germany) so that 4 sections 250 μm apart were present on each slide. The sections were air dried for at least 1 h at RT and stored in boxes at −20 °C until staining was performed.

Prior to the immunofluorescence staining, antigen demasking using 0.01 M sodium citrate solution (pH 9.0) was done in a water bath (80 °C, 30 min). Blocking of nonspecific binding sites was performed for 1 h at RT using phosphate-buffered saline (PBS, pH 7.3) containing 0.2% Triton X-100, 0.02% sodium azide, and 5% normal serum from the species in which the secondary antibody was produced. Incubation with the primary antibody, mouse antiparvalbumin (PV, clone PARV-19, Sigma, Taufkirchen, Germany), or rabbit antivesicular GABA transporter (VGAT, rabbit polyclonal antibody, Synaptic Systems, Göttingen, Germany) diluted 1:1000 with PBS containing 0.5% lambda-carrageenan (Sigma) and 0.02% sodium azide was carried out at 4 °C for 3 days. After washing in PBS (3 × 15 min at RT), the appropriate secondary antibody conjugated with Cy3 (Jackson ImmunoResearch Laboratories, Dianova, Hamburg, Germany) diluted 1:200 in PBS–Carrageenan solution was applied for 2 h at RT. Finally, after a subsequent wash in PBS, cell nuclei were stained for 10 min at RT with bis-benzimide solution (Hoechst 33258 dye, 5 μg/mL in PBS, Sigma), and sections were mounted under coverslips with antifading medium (Fluoromount G, Southern Biotechnology Associates, Biozol, Eching, Germany).

Double staining for PV and VGAT was performed by mixing the primary antibodies at optimal dilutions and using a Cy3-conjugated antimouse and a Cy2-conjugated antirabbit secondary antibody preabsorbed with rabbit and mouse serum proteins, respectively (multiple-labeling grade antibodies, Jackson ImmunoResearch). For a given antigen, all sections were stained in the same solution and kept in screw-capped staining plastic jars (capacity 35 mL, 10 slides, Roth).

Stereological Analysis of PV^{+} Interneurons and Principal Cells

Numerical densities were estimated using the optical disector method as described (Irintchev et al. 2005; Nikonenko et al. 2006). Counting was performed on an Axioskop microscope (Zeiss, Oberkochen, Germany) equipped with a motorized stage and Neurolucida software-controlled computer system (MicroBrightField Europe, Magdeburg, Germany). The volume of the dorsal hippocampus, its subdivisions, and principal cell layers were estimated using spaced-serial sections (250-μm interval) and the Cavalieri principle (Nikonenko et al. 2006). The borders of the hippocampal regions were defined by the nuclear staining pattern (Plan-Neofluar ×10/0.3 objective) according to criteria described by Long et al. (1998). The numerical density of PV^{+} cells was estimated by counting nuclei of immunolabeled cells within systematically randomly spaced optical disectors. The parameters for this analysis were guard space depth 2 μm, base and height of the disector 3600 μm^2 and 10 μm, respectively, distance between the optical disectors 60 μm, objective ×40 Plan-Neofluar ×40/0.75. The same parameters were used for the counting of nuclei in the pyramidal layer except for the base of the disector, which was 900 μm^2, and the space between disectors (30 μm). Nuclei of glial cells in the pyramidal layer were easily recognized and were not counted. Left and right hippocampal areas were evaluated in 4 sections each. All results shown are averaged bilateral values. The counts were performed on coded preparations by one observer.

Light-Microscopic Analysis of Perisomatic Terminals and Principal Cell Size

Estimation of perisomatic puncta and area of principal cell bodies was performed as previously described (Irintchev et al. 2005; Nikonenko et al. 2006). Stacks of images of 1-μm thickness were obtained from different hippocampal subfields in sections double-stained for PV and VGAT using a TCS SP2 confocal microscope (Leica, ×63 oil immersion objective, 1024 × 1024 pixel resolution). One merged image (red and green channels) per cell at the level of the largest cell-body cross-sectional area was used to measure soma area and count individually discernible perisomatic puncta (Supplementary Fig. 5). Numbers of $PV^{+}VGAT^{+}$ and $PV^{-}VGAT^{+}$ puncta were normalized to the perimeter of the cell profile. All measurements were performed using the Image Tool 2.0 software (University of Texas Health Science Center, San Antonio, TX).

Proliferation and Cell Death in the Early Postnatal Hippocampus

Seven-day-old TNR−/− mice and their TNR+/+ littermates (n = 6 per genotype) were anesthetized on ice and sacrificed by decapitation. The brains were fixed by submersion in 4% formaldehyde for 24 h, cryoprotected, frozen, and cut as described above. Tissue sections were stained with rabbit polyclonal antibodies against the proliferation marker Ki67 (1:500, Abcam, Cambridge, United Kingdom) and caspase-3 activated, a marker for apoptotic cells (1:2000, R&D Systems, Minneapolis, MN) using the indirect immunofluorescence procedure described above.

Synaptic Plasticity in the Dentate Gyrus

Because the present study is focused on GABAergic inhibition, an important consideration was that it is difficult to induce dentate gyrus LTP in in vitro preparations without the presence of $GABA_A$ receptor antagonists (Hanse and Gustafsson 1992). A small potentiation induced in vitro without suppression of GABAergic inhibitions represents NR2B-dependent plasticity in immature granule cells rather than NR2B-independent LTP that is induced when $GABA_A$ receptors are blocked (Snyder et al. 2001; own unpublished data). Dentate gyrus LTP in vivo, however, can be induced without these drugs (Errington et al. 1997; Bampton et al. 1999), thus allowing the assessment of the impact of GABAergic inhibition on dentate gyrus LTP. Here, we used a protocol for recordings in anesthetized mice recently established in our laboratory (Stoenica et al. 2006; see Supplementary Material). The stimulating electrode was made of 2 125-μm Teflon-insulated stainless steel wires, whereas the recording electrode was constructed of 75-μm Teflon-insulated tungsten wire or a glass pipette with an opening of approximately 3 μm. The glass pipette was filled with artificial cerebral spinal fluid supplemented with 10-mM bicuculline methiodide (Sigma) to inhibit $GABA_A$ receptors in the vicinity of the recording site (Nosten-Bertrand et al. 1996). The stimulation strength for recordings before and after induction of LTP was selected to provide a population spike of 2–3 mV in experiments without pharmacological treatment or 1–2 mV in experiments with infusion of bicuculline. In the latter case, the stimulus intensity was reduced to avoid polyspiking activity during baseline recordings. The responses were collected every 30 s, and averages of 5 consecutive sweeps were used for analysis. LTP was induced by 6 trains (intertrain interval of 20 s) of 6 bursts (interburst interval of 200 ms) consisting of 6 pulses applied at 400 Hz (Davis et al. 1997). The stimulation intensity used for induction of LTP was 2 times higher than the one used for baseline recordings. Only experiments without rundown of field excitatory postsynaptic potentials (fEPSPs) (>90% of baseline) were included in the analysis.

Behavioral Analysis

Water-Maze Test

A water-maze test was performed on the 9 TNR+/+ and 9 TNR−/− mice that were used for morphological investigations after the test. Before the experiment, mice were familiarized for 2 days to swimming and climbing onto a platform (4 trials per day; 60-s trial maximal duration; 5-min intertrial interval (ITI) as described (Fellini et al. 2006). Then, mice underwent the water-maze test in a 155-cm diameter circular pool

(water at 21 ± 1 °C, made opaque by a nontoxic white paint, 14-cm diameter platform placed 1 cm below the water surface, the center of the platform at 40 cm from the wall, 90-s maximal trial duration; see Supplementary Material). The pool was placed in the center of the experimental room (3.5 × 3.5 m) provided with 6 landmarks approximately 50 × 50 cm in size placed on the walls at a height of 150–180 cm. Mice were started from 6 symmetrical positions in a pseudorandomized order so that the average distance of the starting position from the platform in 2 consecutive trails was always 90 ± 5 cm. After having stayed on the platform for 15 s, mice were returned to their home cage (HC) in a room adjacent to the experimental room and allowed to warm up under red light. All mice were trained over 10 days (days 1–10, 4 trials per day, ITI of 5 min). The platform was located in the center of the target quadrant (4 platform positions placed in the center of the 4 quadrants were counterbalanced within each genotype). A probe trial was performed 5 min after the last training trial on day 8: The platform was removed, and mice were allowed to swim for 60 s. To avoid extinction, the probe trial was followed by 4 learning trials on days 9 and 10 with the platform located in the previous position. On days 11 and 12, mice underwent a reversal learning protocol. On day 11, mice underwent 2 trials with the platform located at the position as on days 1–10 and were then trained in 4 trials with the platform placed at the center of the quadrant opposite to the previous target quadrant. Because reversal learning started 5 min after the last learning trial, memory of the first platform position could potentially interfere with the learning of the new platform location. It has been suggested that functional hippocampus-dependent episodic-like memory is required to avoid this interference and allow fast reversal learning (Wood et al. 2000). On day 12, mice were trained over 4 trials with the platform located as in trials 2–6 on day 11. To test whether mice had learned to search for the platform in the new position, a probe trial was performed 5 min after the last trial on day 12.

Trial-to-Criterion Protocol

Mice (13 TNR+/+ and 13 TNR−/− mice) were trained under similar conditions as those described for the water-maze test. To evaluate the reversal learning capacities, a "trial-to-criterion" protocol (Chen et al. 2000) for 5 consecutive platform positions was used. Each mouse was trained, for up to 9 trials per day (5-min ITI), to find a platform location until it reached a determined criterion (3 consecutive trials with an average escape latency ≤ 15 s) before being trained for a new location on the next day. Thus, a mouse was trained for one platform location over a minimum of 4 trials (the escape latency of the first trial was not taken in consideration) up to an open number of trials. All mice were tested until they had reached the criterion for 5 different platform locations. The number of trials required to reach the criterion was evaluated. The first 15 s of the first trial with the platform positions 2–5 were used to measure the spatial selectivity for the previous position of the platform (e.g., the first trial with the platform in position 2 was used as probe trial for the platform position 1).

Test for Olfactory Learning and Reversal Learning

Mice (11 TNR−/− and 11 TNR+/+ mice) were exposed to 2 odors (A and B) and trained to learn that only odor A was associated with a food reward. Learning abilities were studied in a probe trial during which the preference for odor A versus odor B in the absence of the reward was tested. During the reversal learning protocol, mice had to learn that odor B, and not odor A, was associated with the reward. The experiment was performed under free choice conditions to minimize the influence of factors related to stress or state anxiety on the performance of the mice. Mice were single housed in Plexiglas cages (13 × 20 cm and 23 cm high) equipped with a small lockable hole (4 cm in diameter) at the bottom of one of the walls. First, mice were habituated for 4 days to emerge from the HC to collect a piece of chocolate (1.4 g) placed in the proximity of the door. Then mice underwent 4 pretraining trials on 4 consecutive days during which they were trained to emerge from the HC into a rectangular open field (75 × 90 cm with 30-cm high walls). Four Petri dishes (diameter of 4.5 cm, 1 cm high) containing one piece of chocolate each were placed along each of the 2 90-cm walls at a distance of 4.5 cm from each other. The open field was surrounded by a black curtain and illuminated (5 lx) with a vertically positioned white bulb. Each pretraining trial started when the door was opened, and latency to enter the open field with 4 paws (emergence latency), latency to approach the first chocolate pellet, and latencies to eat the first and last chocolate pellet were recorded. Only mice eating all the 8 pieces of chocolate within 10 min during the last pretraining trial were used for further training for olfactory learning. The protocol for olfactory learning comprised a first learning trial on day 1, a probe trial on day 2, second and third learning trials on days 3 and 4, respectively, a probe trial on day 5, a reversal learning trial on day 6, and a probe trial on day 7. During the learning trials, Petri dishes were filled with sand aromatized with either nutmeg (5% in sand) or cinnamon (5% in sand). Among the 4 Petri dishes along the same wall, 2 were aromatized with nutmeg and 2 with cinnamon and placed in the order nutmeg–cinnamon–nutmeg–cinnamon along the left wall from the HC and cinnamon–nutmeg–cinnamon–nutmeg along the opposite wall. All learning trials were performed as in the pretraining trials with the only difference being that a piece of chocolate was placed only in the 4 dishes having a determined odor: To avoid a bias caused by innate aversion or attraction to one odor, dishes with nutmeg were baited for 6 mice per genotype, whereas dishes with cinnamon were baited for 5 mice per genotype. The probe trials were performed to test the preference of the mice for the previously baited odor in the absence of the chocolate: Sixteen dishes were placed along the walls of the open field with the most proximal dishes placed on the left and right sides of the door of the HC at a distance of 5 cm (Fig. 7C). All 8 dishes on the left side from the HC were filled with cinnamon, whereas those on the right side with nutmeg. The probe trial, initiated when the mice had entered the open field with 4 paws, lasted 60 s. Time spent in risk assessment from the HC toward the open field, emergence latency, latency to approach the first cinnamon and nutmeg dish, and number of approaches to the cinnamon and nutmeg dishes (defined as when the mouse's nostrils were over the dish) were scored.

Spontaneous Alternation and Win-Shift Tests

Seventeen TNR+/+ and 18 TNR−/− mice were tested in the spontaneous alternation and win-shift paradigms using a T-maze. The spontaneous alternation test was performed as described (Morellini and Schachner 2006). The T-maze consisted of 3 arms of the same size (34 × 5 cm and 30 cm high): 2 opposing arms and one central arm, made of Plexiglas and connected such as to make a T. Sliding doors were placed at the entrance of the opposing arms and at 10 cm from the dead end of the central arm. Mice were tested over 2 days, 1 session per day and 14 trials per session with an ITI of 5 s. Each session was started by placing the mouse at the dead end of the central arm with the door closed. After 5 s, the door was opened, and the mouse was allowed to freely enter one of the 2 opposing arms. Once the mouse had entered one arm, access to the opposite one was occluded by the sliding door. As the mouse returned to the dead end of the central arm, it was confined there for 5 s before starting the next trial. Data were analyzed as percentage of alternations over all trials.

The win-shift test was designed to test working memory under free choice conditions in order to minimize the influence of factors related to stress or state anxiety on the performance of the mice. The mice could freely emerge from their HC and enter the central arm of a T-maze. Following a win-shift criterion ("if you win, then shift"), at each trial a food reward was located in the arm opposite to that where it had been previously found. To familiarize the mice with the reward and the testing conditions, mice underwent a pretraining protocol before being tested in the win-shift test (see Supplementary Material). After the pretraining protocol, mice were trained in the win-shift test for 4 days, 1 session per day and 14 trials per session. On training days 1 and 2, the ITI was 15 s, and on days 3 and 4 the ITI was 60 s. The win-shift test was performed in the T-maze used during the pretraining protocol with the difference that one small dispenser that could contain one pellet of chocolate (an opaque Plexiglas cylinder with a diameter of 5 and 5 mm high) was placed 2 cm from the edge of both opposite arms. To equalize the smell of chocolate in the 2 opposite arms, between the dispensers and the edges of the arms, 5 chocolate pellets were placed behind a metallic grid, so that a mouse in the T-maze could smell but not eat the pellets behind the grid. Mice underwent 4 training sessions of 14 trials performed on 4 consecutive days. The test was started by

opening the door of the HC so that a mouse could freely enter the central arm end explore one of the opposing arms. As the mouse entered one of the opposing arms, the door occluding the opposite arm was closed so that mice could only return into the central arm and finally into their HC. In the first trial of each session, the dispensers in both arms were baited. After the mouse had entered one arm, eaten the chocolate pellet, and returned to its HC, it was confined thereby keeping the door closed for 15 s on training days 1 and 2, and 60 s on days 3 and 4. The second trial was started by opening the door again. During trials 2–14, mice had to find the chocolate following a win-shift rule, namely the chocolate was only in the dispenser in the arm opposite to the one where the mouse had previously found it. The test was performed in darkness and videorecorded using an infrared camera. Data were analyzed as percentage of correct choices over all trials. In addition to number of correct choices, emergence latency (time required to enter into the T-maze with 4 paws from the moment when the door was opened), latency to eat the chocolate (time required to eat the chocolate after the mouse had entered the T-maze), and duration of each trial (measured from the moment a mouse had entered the central arm to the moment it returned into the HC) were recorded.

Step-Through Passive Avoidance Test

Twelve mice per genotype were tested. A 2-compartment box equipped with a grid floor was used. The box was made of white plastic with a sliding door (5 × 5 cm) connecting the 2 compartments. One compartment (25 × 21 and 30 cm high) was illuminated (50 lx), whereas the other (25 × 21 and 30 cm high) remained dark (<0.5 lx). On the first day, mice were placed into the illuminated compartment. After 1-min, the sliding door was opened. After the mouse had encountered the open door for the first time, the latency to enter the dark compartment was measured. When the mouse had entered the dark compartment with 4 paws, the door was closed, and a foot shock (1 s, 0.25 mA) was delivered. Mice were then immediately returned to their HCs. Retention was tested 24 h later by repeating the whole procedure, with the exception that the mice did not receive any foot shock. Mice were given 300 s to enter the dark compartment after which the test was interrupted.

Fear Conditioning Test

The test was performed as described (Morellini and Schachner 2006). The conditioned stimulus consisted of a constant high-pitch tone cue (85 kHz, 80 dB, and 20 s). The unconditioned stimulus consisted of an electric foot shock (0.34 mA, 2 s) elicited from the grid floor. At conditioning, mice were placed into the conditioning chamber and received 2 tone-foot shock presentations. The following protocol was used: 0-s recording start, 120-s tone on, 138-s shock on, 140-s tone and shock off, 170-s tone on, 188-s shock on, 190-s tone and shock off, and 240-s recording end. Mice were then tested for memory retrieval in the shock chamber (context) and in an unfamiliar cage (new cage). When retrieval was performed in the conditioning chamber (context), all conditions were kept the same as for the conditioning protocol, except that the mice did not receive any shock. Potential similarities in olfactory cues between the context and new cage were reduced by additionally cleaning the new cage with a soap solution. Twenty-one hours after conditioning, mice were tested for retention in the new cage and 6 h later in the context (24-h retention tests). Mice were tested again for retention on days 8 and 9 (1-week retention tests); to avoid possible bias due to the temporal order of the tests, half of the mice from each genotype were tested in the context on day 8 and in the new cage on day 9, whereas the other half were tested on day 8 in the new cage and on day 9 in the context.

New Cage and New Object Tests

Because performances in the tests for cognitive abilities could be influenced by novelty-induced behavior and anxiety, we performed the new cage and new object tests as described (Brandewiede et al. 2005; Morellini and Schachner 2006) on the same mice that have then undergone the water-maze test. Mice were taken from their HC, placed into a new cage (38 × 22 × 15 cm) with fresh bedding, and videorecorded for 5 min. They were then left undisturbed in the new cage. After 24 h, the behavior in the new cage (now familiar to the mouse) was videorecorded for 5 min before introducing a new object into the cage. The new object consisted of a plastic water bottle (7 ×7 cm and 10 cm high) for rodents with the bottom cut-off and with an entrance of 3 × 4 cm on one side. The bottle was placed into the cage with the entrance facing the center of the cage. Behavior was videorecorded for 5 min after the new object had been introduced into the cage.

Analysis of Behavioral Parameters

All experiments were videorecorded and analyzed automatically with the tracking system Ethovision (Noldus) and manually by a blinded trained experimenter using The Observer software (Noldus) as described (Freitag et al. 2003; Morellini and Schachner 2006).

Statistical Analysis

All data are presented as group mean values with standard error of mean (SEM). Two-tailed parametric and nonparametric tests were used to analyze the data as indicated in the Results and Figure legends. The accepted level of significance was 5%. The nonparametric Spearman's test was used to analyze correlations between morphological and behavioral data sets. To restrict the number of correlations, the most relevant behavioral parameters were selected using principal components analysis as described (Morellini and Schachner 2006; Supplementary Material).

Results

Hippocampal Subfield Volumes, PV⁺ Interneurons, and Principal Neurons

We first analyzed the hippocampus of TNR–/– mice and TNR+/+ littermates morphometrically to evaluate the anatomical consequences of the mutation. We found an overall tendency for enlargement of the dentate gyrus and cornu ammonis in TNR–/– mice compared with TNR+/+ mice (Fig. 1*A*,*B*). The differences between the genotypes for different subfields and layers ranged between 10% and 36% and were statistically significant for the volume of the dentate gyrus (Fig. 1*A*) and the volume of the pyramidal cell layers in CA3 and CA1 subfields of the hippocampus (Fig. 1*B*). No differences were found for the ratios of principal cell layer volumes to total subfield volume (not shown). In contrast to the hippocampus, the whole brain mass and volume were similar in TNR–/– and TNR+/+ mice (401 ± 19 and 415 ± 15 mg, 390 ± 13 and 389 ± 23 mm^3, respectively, $P > 0.05$, *t*-test).

TNR is expressed by PV^+ interneurons, a major subpopulation of GABAergic interneurons in the hippocampus, and accumulates in the perineuronal nets surrounding these cells. Therefore, we expected that the constitutive ablation of TNR could affect this interneuron population. Indeed, we found that the numerical densities (number per unit volume) of PV^+ cells were increased in all areas of the hippocampus of TNR–/– compared with TNR+/+ mice (Fig. 2*B*–*E*, "Density"). The differences between group mean values were most prominent in the dentate gyrus (Fig. 2*B*, "Density") and CA3 (Fig. 2*C*, "Density"). As a consequence of higher cell densities and, in part, volumes of the hippocampal subdivisions in TNR–/– mice, the total number of PV^+ interneurons was higher in TNR–/– compared with TNR+/+ mice (Fig. 2*B*–*E*, "Number"). The finding of a pronounced effect of the TNR deficiency on the size of the PV^+ cell population raised the question whether interneuron cell body area was also influenced by the mutation. We measured soma areas of randomly sampled PV^+ interneurons and found no difference between genotypes for any of the hippocampal subfields (Supplementary Fig. 1).

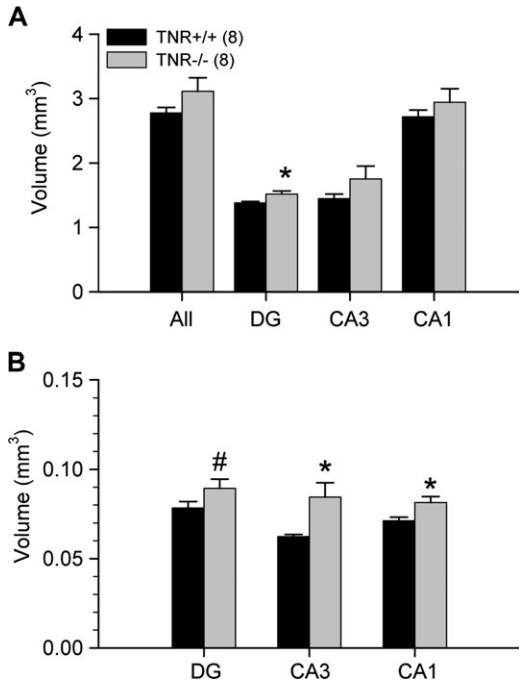

Figure 1. Increased hippocampal volumes in TNR−/− mice. (*A*) Volumes of the whole hippocampus (All), dentate gyrus (DG), and CA3 and CA1 subfields. Multiplication factor 2 is used to adapt values of the DG, CA3, and CA1 to the scaling. (*B*) Volumes of principal cell layers in the different hippocampal subfields. Numbers of animals studied per group are indicated in brackets. $^*P < 0.05$, $\#P = 0.12$ (*t*-test).

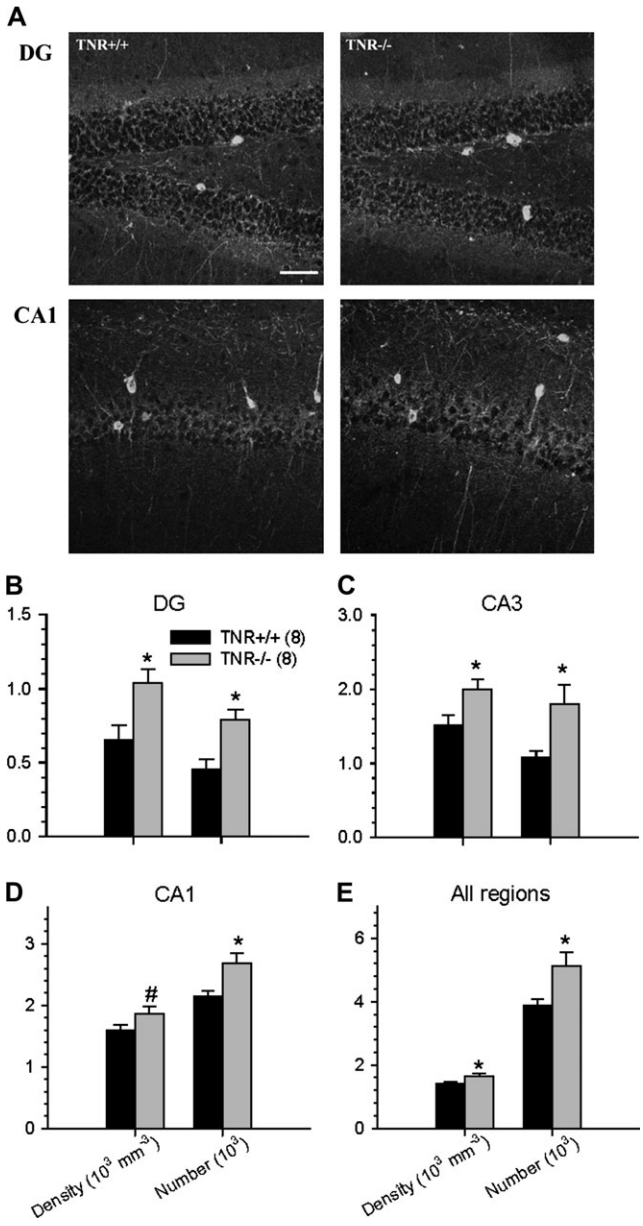

Figure 2. Increased numbers and densities of interneurons in TNR−/− mice. (*A*) Representative images of immunostainings for PV in the CA1 and DG of TNR+/+ (left panels) and TNR−/− (right panels) mice. Scale bar: 40 μm. (*B–E*) Numerical density (Density) and total number (Number) of PV^+ cells in the dentate gyrus (*B*), the CA3 (*C*) and CA1 (*D*) regions and the whole dorsal hippocampus (*E*) of TNR+/+ and TNR−/− mice. The number of animals studied per group is indicated in brackets in (*B*). $^*P < 0.05$, $\#P = 0.12$ (*t*-test).

Because the function of hippocampal circuits is tightly regulated by the balance between inhibition and excitation, we next analyzed cell densities of excitatory neurons (pyramidal and granule cells) in the 3 hippocampal areas using nuclear staining to identify the cells. The density of principal cells was similar in all hippocampal areas of TNR–/– and TNR+/+ mice (Fig. 3*A–C*, "Density"). However, the total number of pyramidal neurons in CA3 and CA1 was significantly higher in TNR–/– versus TNR+/+ mice (Fig. 3*B,C*, "Number"). A tendency for a higher number of granule cells in the dentate gyrus of TNR–/– mice compared with TNR+/+ mice was also found (Fig. 3*A*, "Number"). In addition to their numerical increase, pyramidal neurons in the cornu ammonis of TNR–/– mice had larger cell body size than pyramidal neurons in TNR+/+ mice (Fig. 3*B,C*, "Soma area"). The total number of PV^+ interneurons and pyramidal cells in CA1 and CA3 was proportionally increased in TNR–/– mice and, thus, the ratio of PV^+ to pyramidal cells was not different from TNR+/+ mice (Fig. 3*B,C*, "PV^+/principal cells"). In the dentate gyrus, however, due to a larger increase in the number of PV^+ cells compared with granule cells, this ratio was higher in TNR–/– compared with TNR+/+ mice (Fig. 3*A*, "PV^+/principal cells"), suggesting that a single principal neuron is innervated by a higher-than-normal number of inhibitory interneurons.

To test whether morphological alterations in different hippocampal subfields of TNR–/– mice are linked with each other, we performed a principal component analysis of the morphological parameters. This approach allows analysis of multiple correlations between parameters and detection of general factors that account for the variability in the data. We identified 4 factors that accounted for 86% of the overall variability (Table 1). All measurements related to the CA3 (with the exception of CA3 volume that loaded only weakly) and number of PV^+ cells in CA1 strongly loaded under factor 1: Volume of the granule cell layer in the dentate gyrus and number of principal cells in dentate gyrus loaded under factor 2; volume, number of PV^+ cells and ratio of PV^+ to pyramidal cells of the dentate gyrus loaded under factor 3; volume of CA1 and CA3; volume of CA1 pyramidal cell layer and number of principal cells in CA1 loaded under factor 4. Thus, the segregation of morphological parameters into subfield-specific clusters represented by different factors suggests that structural characteristics of the hippocampal subfields (dentate gyrus, CA3, and CA1), such as subfield volume and number of

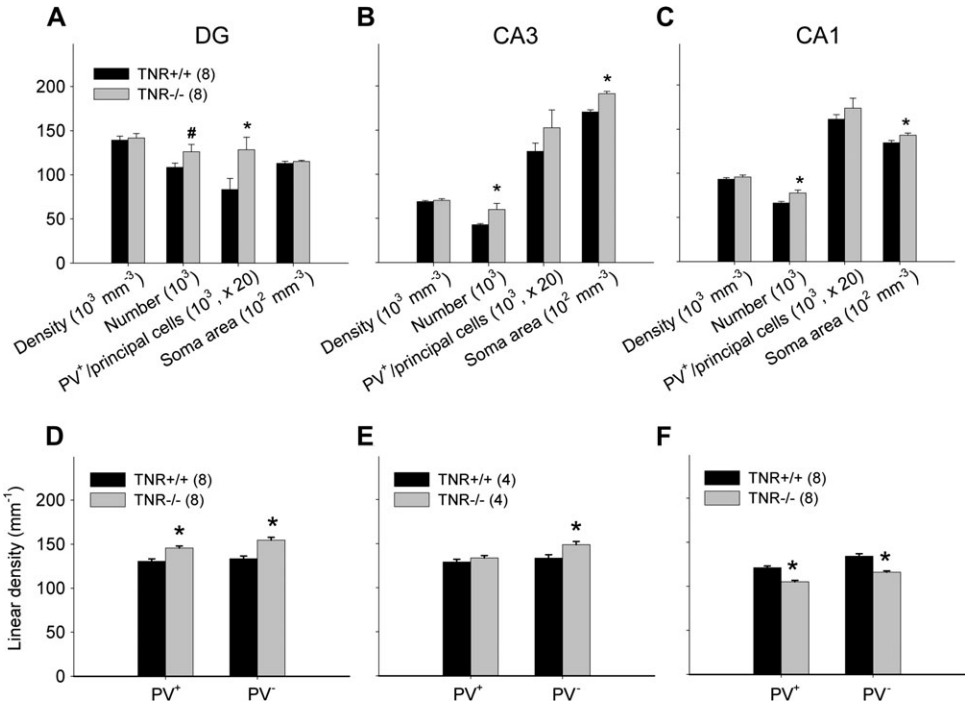

Figure 3. Enhanced ratio of PV^+ to principal cells and densities of inhibitory perisomatic puncta around granule cells. Numerical density (Density) and total number of principal cells (Number), ratio of PV^+ to principal cells and principal cell soma size (Soma area) in the dentate gyrus (*A*), CA3 (*B*), and CA1 (*C*) region of the dorsal hippocampus of TNR+/+ and TNR−/− mice. Multiplication factors are used to adapt some values to the scaling. $^*P < 0.05$, $\#P = 0.10$ (*t*-test). (*D–F*) Linear densities of PV^+VGAT^+ ("PV^{++}"), PV^-VGAT^+ ("PV^{-+}") perisomatic terminals in the dentate gyrus (*D*), CA3 (*E*), and CA1 (*F*) of the hippocampus. $^*P < 0.05$ (*t*-test). The number of animals studied per group for (*A–F*) is indicated in brackets in (*A*) The number of cells/animals studied per group for (*D–F*) is indicated in brackets in (*E*). Group mean values of the parameters are calculated from individual mean values. $^*P < 0.05$ (*t*-test).

Table 1
Factor loadings for morphological parameters

	Factor 1	Factor 2	Factor 3	Factor 4
DG (vol)			0.69	
DG-PV+ cells (*n*)			0.84	
DG granular cell layer (vol)		0.91		
DG principal cells (*n*)		0.95		
DG PV+/principal cells			0.88	
CA3 (vol)	0.50			0.77
CA3-PV+ cells (*n*)	0.69			
CA3 pyramidal cell layer (vol)	0.93			
CA3 principal cells (*n*)	0.94			
CA3 PV+/principal cells	0.71			
CA1 (vol)				0.83
CA1-PV+ cells (*n*)	0.74			
CA1 pyramidal cell layer (vol)				0.64
CA1 principal cells (*n*)				0.75
CA1 PV+/principal cells	0.59			

Note: DG: dentate gyrus; *n*: number; and vol: volume. Loadings < 0.5 are not shown.

principal cells and PV^+ interneurons, are not significantly interdetermined. This idea is in agreement with the fact that the effects of TNR ablation were subfield- and cell type-specific.

Perisomatic Inhibitory Inputs to Principal Neurons

In search of further structural evidence that the balance between inhibition and excitation is altered in the hippocampus of TNR–/– mice, we analyzed synaptic coverage of principal neurons in the dentate gyrus, CA3, and CA1 using immunohistochemistry and confocal image analysis. As there are 2 major subtypes of perisomatic GABAergic input to the cell bodies of principal cells, those provided by PV^+ cholecystokinin-negative basket cells and by PV-negative (PV^-) cholecystokinin-positive basket cells (Freund 2003), we identified one of these types of terminals as positive for both PV and VGAT and the other one as positive for only VGAT (Nikonenko et al. 2006). In the dentate gyrus of TNR–/– mice, in which the ratio of PV^+ interneurons to granule cells was increased, densities of both PV^+ and PV^- perisomatic puncta were higher compared with TNR+/+ mice (Fig. 3*D*), whereas there was no difference in granule cell soma area between the genotypes (Fig. 3*A*, "Soma area"). In the CA1 region, we found that fewer perisomatic terminals, both PV^+ and PV^-, surrounded the CA1 pyramidal cell bodies in TNR–/– mice compared with TNR+/+ mice (Fig. 3*F*). These observations are in agreement with previous electron microscopic findings of reduced total perisomatic input to CA1 pyramidal cells in young TNR–/– mice (Nikonenko et al. 2003). In the CA3 region of TNR–/– mice, the density of PV^+ perisomatic puncta was normal, whereas the density of PV^- terminals was slightly increased compared with TNR+/+ mice (Fig. 3*E*).

Proliferation and Cell Death in the Early Postnatal Hippocampus

TNR is expressed during the postnatal development of the hippocampus (Fuss et al. 1993; Supplementary Fig. 2) and may influence, as suggested by recent in vitro data (Liao et al. 2008), the proliferation and differentiation of stem–progenitor cells and their progeny. We, therefore, analyzed whether increased neuronal cell numbers in adult TNR–/– mice were due to increased cell proliferation or decreased apoptotic cell death. We used hippocampal sections from 7-day-old mice, an age at

which both neurogenesis and cell death of principal neurons and interneurons, especially in the dentate gyrus, occur at high levels (Reznikov 1991; Madden et al. 2007). We stained the sections for the proliferating cell antigen Ki67 and activated caspase-3, a marker for apoptotic cells. The density of caspase-3^+ cells in the hippocampus was 20 ± 1.8 mm^{-2} in TNR+/+ mice versus 11 ± 0.54 mm^{-2} in TNR–/– mice ($P < 0.01$, *t*-test). Conversely, the number of $Ki67^+$ cells was similar in the 2 genotypes (278 ± 8.5 mm^{-2} in TNR+/+ mice vs. 294 ± 11 mm^{-2} in TNR–/– mice, $P > 0.05$, *t*-test). Thus, TNR ablation decreases cell death in the hippocampus during early postnatal development, without affecting proliferation.

Synaptic Transmission and Plasticity in the Dentate Gyrus

Based on the morphological results that indicate elevated perisomatic GABAergic coverage on granule cells in the TNR–/– dentate gyrus, we investigated whether synaptic properties are altered in this region under TNR ablation. We performed in vivo electrophysiological recordings of LTP that, in contrast to in vitro approaches, allow the assessment of LTP under more physiological conditions and, in particular, in the absence of pharmacological disinhibition (Errington et al. 1997). Theta-burst stimulation elicited a robust LTP in TNR+/+ mice, as previously reported for different mouse strains (Errington et al. 1997; Bampton et al. 1999). Three hours after induction of LTP, the magnitude of potentiation in the slope of fEPSPs was 123 ± 3.6% in TNR+/+ and 108 ± 5.3% in TNR–/– mice ($P < 0.05$, *t*-test; Fig. 4*B*). Also short-term potentiation (STP), that is, increase of fEPSP immediately after theta-burst stimulation, was strongly reduced in TNR–/– mice (Fig. 4*B*), suggesting that induction of LTP is impaired in this mutant. However, the magnitude of population spike amplitude potentiation was 231 ± 25% in TNR+/+ mice, whereas it was 362 ± 38% in TNR–/– mice ($P < 0.01$, *t*-test; Fig. 4*A*). To analyze changes in excitability in more detail, we estimated the levels of EPSP-spike (E-S) potentiation as a ratio between population spike amplitudes measured 3 h after and before induction of LTP for fEPSPs with a fixed slope of fEPSPs (corresponding to the one measured after induction of LTP). TNR–/– mice had higher magnitude of E-S potentiation (123 ± 21%) than TNR+/+ mice (77 ± 9%) ($P < 0.05$, *t*-test). Thus, 3 h after theta-burst stimulation, potentiation of population spikes, and E-S potentiation were larger, whereas potentiation of fEPSPs was substantially impaired in TNR–/– mice compared with TNR+/+ mice.

To test the possibility that abnormal LTP in TNR–/– mice is due to elevated GABAergic inhibition, as suggested by our

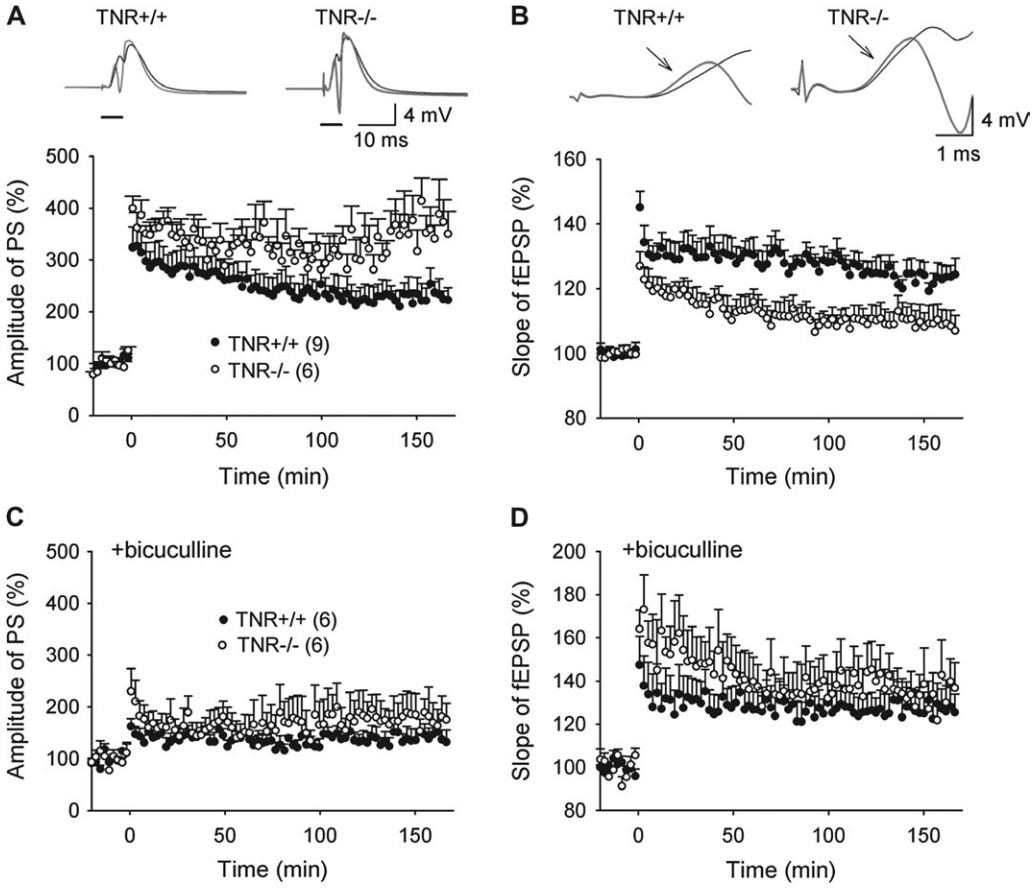

Figure 4. Impaired LTP of fESPSs in the dentate gyrus of TNR−/− mice and its restoration to TNR+/+ levels by suppression of GABAergic inhibition. (*A,B*) LTP was induced without pharmacological manipulation. (*C,D*) LTP was induced during infusion of 10 mM bicuculline. Data represent mean + SEM of population spike (PS) amplitude (*A,C*) and slope of fEPSPs (*B,D*) expressed in % regarding the baseline (time from −20 to 0 min). Theta-burst stimulation (applied at time 0) elicited a robust LTP in TNR+/+ and TNR−/− mice. Examples of responses collected before and immediately after induction of LTP are shown above the LTP profiles. Horizontal bars in (*A*) indicate time intervals that are shown with a higher resolution in (*B*). Arrows in (*B*) point to the initial phase of fEPSPs where the measurements of slope were made. The number of animals studied per group is indicated in brackets.

morphological data, we attempted to restore LTP by pharmacological suppression of $GABA_A$ receptors. After infusion of the $GABA_A$ receptor antagonist bicuculline via the recording pipette, which leads to a local disinhibition in the dentate gyrus (Nosten-Bertrand et al. 1996), we observed no difference in basal synaptic transmission between genotypes. The potentiation of the population spike amplitude was significantly smaller in both genotypes compared with pharmacologically untreated mice. Three hours after induction of LTP, the magnitude of population spike amplitude potentiation was 144 ± 20% in TNR+/+ and 175 ± 35% in TNR−/− mice ($P > 0.05$, *t*-test; Fig. 4*C*). A similarly strong reduction in population spike amplitude potentiation in the presence of bicuculline has been reported for wild-type mice (Nosten-Bertrand et al. 1996). STP in the presence of bicuculline was 147 ± 13% in TNR+/+ and 164 ± 8.7% in TNR−/− mice ($P > 0.05$, *t*-test; Fig. 4*D*). Three hours after induction, the magnitude of LTP was 126 ± 10% in TNR+/+ and 132 ± 9.8% in TNR−/− mice ($P > 0.05$, *t*-test; Fig. 4*D*). Thus, bicuculline fully restored STP and LTP of fEPSPs in TNR−/− mice, supporting the view that the deficit in synaptic plasticity in the dentate gyrus of TNR−/− mice is due to enhanced GABAergic inhibition in this region.

Water-Maze Test

We then assessed the effects of functional and structural aberrations in the dentate gyrus on the cognitive abilities of TNR−/− mice. The water-maze test indicated that both genotypes learned and remembered equally well the position of a hidden platform by means of a spatial searching strategy. However, when the platform was relocated to a new position in the maze, TNR−/− mice were faster in finding the platform, suggesting that they could change their searching strategy more flexibly compared with TNR+/+ mice (Fig. 5*A*,*B*).

Daily mean escape latency and distance moved to reach the platform were analyzed from the learning trials of the first and second platform positions (learning and reversal learning, respectively). Because the same results were obtained for distance moved and escape latency, for brevity, we present here the data on distance moved which, on the contrary to escape latency, is not biased by swimming velocity or floating. The data relative to escape latency are shown in Supplementary Fig. 6. Mice of both genotypes learned to find the first platform at the end of training with no differences between genotypes (Fig. 5*A*). Although TNR−/− mice tended to find the platform faster compared with TNR+/+ mice on day 2, the effect of the interaction between "Genotype" and "Day" on distance moved

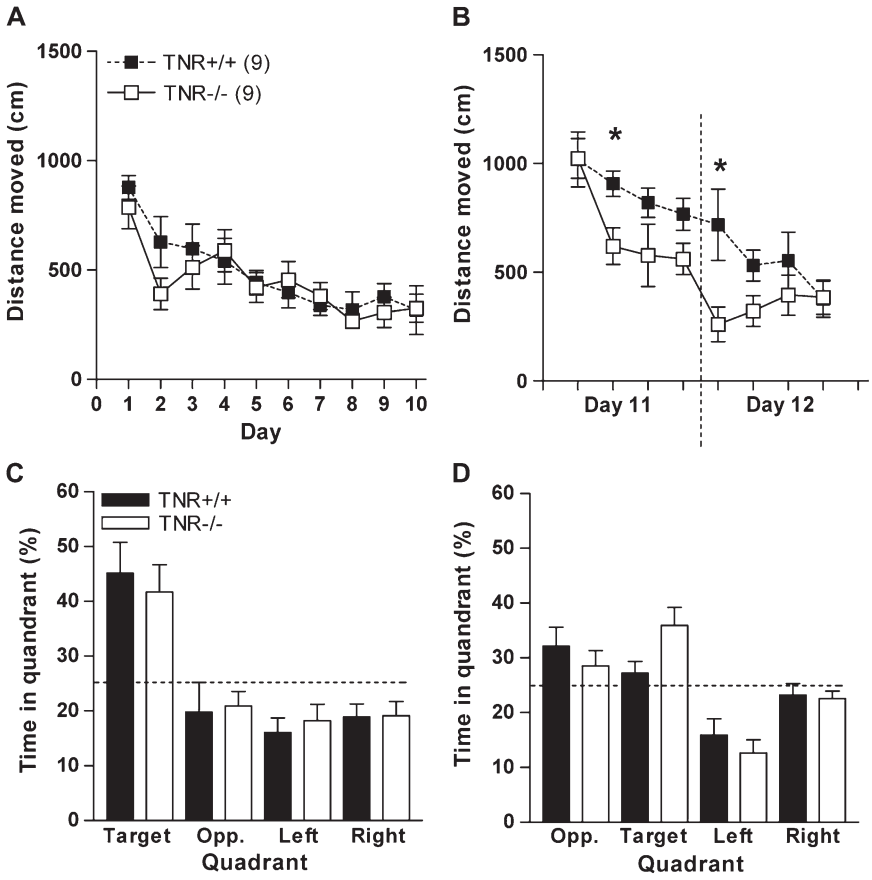

Figure 5. TNR−/− mice are faster during reverse learning in the water-maze test. (*A*) Learning success was evaluated by distance moved (calculated as mean of the daily 4 trials) to find the platform. Both genotypes learned the first platform position (days 1–10) equally well. TNR−/− mice covered shorter distances than TNR+/+ mice to finding the platform on day 11 when the platform was located in a position opposite to the one where it was located on days 1–10. *$P < 0.05$ comparison between TNR+/+ and TNR−/− mice on day 11 (Newman–Keuls test after 2-way ANOVA for repeated measurements). (*B*) TNR−/− mice covered shorter distances during the first trial of the second reversal learning day (day 12) compared with TNR+/+ mice. *$P < 0.05$ (Mann–Whitney test). (*C*) Both genotypes showed a significant preference for the target quadrant compared with the other 3 quadrants in the probe trial on day 8 (effect of quadrant, $F_{3,42} = 14.3$; $P < 0.001$). (*D*) In the probe trial on day 12, neither genotype showed a clear preference for a specific quadrant, although they tended to stay more in the quadrants of the old and new target position compared with the other 2 quadrants. (*C*,*D*) The horizontal dotted line indicates the chance level (25%) to stay in 1 of the 4 quadrants. The number of animals studied per group is indicated in brackets in (*A*).

between days 1 and 10 was not significant ($F_{9,126}$ = 1.1; P > 0.05), whereas there was a significant effect of Day ($F_{9,126}$ = 11,7; P < 0.001), indicating that mice of the 2 genotypes learned equally well. Three-way analysis of variance (ANOVA) for repeated measurements performed on distance moved during the first and second days of reversal learning, days 11 and 12, respectively, indicated a significant effect of the interaction between Genotype, Day, and Trial ($F_{3,42}$ = 3.2; P < 0.05): Post hoc analyses showed that TNR–/– mice swam shorter distances to find the platform compared with TNR+/+ mice in trial 2 on day 11 and trial 1 on day 12 (Fig. 5*B*). In the probe trial performed on day 8 of learning, TNR+/+ and TNR–/– mice selectively searched for the platform at the correct location, indicating good spatial memory in both genotypes (Fig. 5*C*). In the probe trial performed at the end of the reversal learning protocol, no significant preference for any of the quadrants was detected, although TNR+/+ and TNR–/– mice tended to stay more in the quadrants of the new and old platform positions than in the other 2 quadrants (Fig. 5*D*).

Correlations between Behavioral and Morphological Data

To test the hypothesis that the altered behavior of TNR–/– mice in the water-maze test is related to the structural alterations observed in the hippocampus, correlation analyses were performed between morphological estimates and 2 behavioral parameters: distance moved in the first trial of the second day of reversal learning and time spent at the target zone during the probe trial on day 8 of learning. These behavioral parameters were selected by principal components analysis as variables best characterizing the 2 major behavioral aspects (i.e., reversal learning and long-term memory) detected in the water-maze test (see Supplementary Material). Distance moved in the first trial of the second day of reversal learning (day 12) was found to be most representative for the ability of the mice to quickly acquire information relevant to the new platform position. Calculated for TNR+/+ and TNR–/– mice separately, this parameter correlated negatively, for both genotypes, with the volume of the dentate gyrus (Fig. 6*A*), number of granule cells (Fig. 6*B*), ratio between PV^+ cells and granule cells (Fig. 6*C*), density of PV^+ perisomatic terminals (Fig. 6*D*), and volume of the granule cell layer (Fig. 6*E*). These correlations were highly significant also when calculated for all animals, both TNR+/+ and TNR–/– mice, with coefficients of correlation r = –0.86 for dentate gyrus volume (P < 0.001), r = –0.81 for granule cell numbers (P < 0.001), r = –0.72 for ratios of PV^+ cells to granule cells (P < 0.01), r = –0.77 for density of PV^+ perisomatic terminals (P < 0.001), and r = –0.83 for granule cell layer volume (P < 0.001). These findings suggest that faster reversal learning is associated with larger volume of the dentate gyrus and its granular layer, higher numbers of granule cells, higher ratios of PV^+ to granule cells, and higher densities of PV^+ terminals on granule cell somata. Similar results were obtained when the behavioral parameter escape latency in the first trial of the second day of reversal learning, day 12, was used (Supplementary Fig. 7). The second behavioral parameter used for correlation analysis was time spent at the target zone during the probe trial on day 8 of learning, which was considered characteristic of the ability of the mice to memorize the precise location of the platform. This parameter positively correlated with the volume of the granule cell layer (Fig. 6*F*, overall r = 0.69; P < 0.01) and with the numbers of granule cells (Fig. 6*G*, overall r = 0.66; P < 0.01). In contrast to the dentate gyrus, time spent at the target zone correlated negatively with the volume of CA3 (Fig. 6*H*, overall r = –0.85; P < 0.001) and the CA1 subfield (Fig. 6*I*, overall r = –0.68, P < 0.01).

We then performed a correlation between the behavioral parameters and the standardized scores calculated for the individual mice for the 4 factors generated from the principle component analysis of the morphological parameters (see Table 1). We found significant correlations between time spent in target zone during the probe trial on day 8 and factors 2 (under which number of granule cells and volume of granule cell layer loaded) and 4 (under which volume of CA1 and CA3, volume of CA1 pyramidal cell layer and number of principal cells in CA1 loaded), and between distance moved in the first trial of the second day of reversal learning and factor 3 (under which volume, number of PV^+ cells, and ratio of PV^+ to pyramidal cells of the dentate gyrus loaded) (Supplementary Fig. 8). Thus, the ability of mice to memorize spatial information was linked to the structural parameters of the dentate gyrus, CA1, and CA3 subfields, whereas the rate of reversal learning correlated with several structural parameters of the dentate gyrus. No correlation was detected between any morphological measurement and the behavioral parameters obtained from the new cage and new object tests (Supplementary Table 1).

Trial-to-Criterion Protocol

To investigate whether the better performance of TNR–/– mice during reversal learning in the water-maze test was due to enhanced reversal learning abilities or due to a more flexible use of alternative nonspatial searching strategies, a new cohort of mice was tested in the trial-to-criterion protocol in which multiple platform positions are learned consecutively. TNR–/– mice learned the new platform positions significantly faster and showed higher spatial preference for the previously learned platform position compared with TNR+/+ mice. Two-way ANOVA showed a significant effect of Genotype ($F_{1,24}$ = 8.23, P < 0.01), of Platform position ($F_{4,96}$ = 18.56, P < 0.001), and of the interaction between Genotype and Platform position ($F_{4,96}$ = 2,98, P < 0.5). Post hoc analyses indicated that TNR–/– mice needed fewer trials to reach the criterion for platform positions 2, 3, and 5 (Fig. 7*A*). The analysis of the first 15 s of the first trials with the platform in positions 2–5 was used to measure the spatial preference for platforms 1–4, respectively (e.g., the first 15 s of the first trial with the platform in position 2 was used to analyze the spatial preference for the platform position 1). Both genotypes preferentially searched in the proximity of the previous platform position as indicated by the fact that the percentage of time in the target quadrant was significantly higher than the chance level of 25% (Fig. 7*B*). This result confirmed that once mice had reached the learning criterion, they learned the spatial position of the platform and did not use an alternative strategy such as circling or looping (Whishaw et al. 1995). Two-way ANOVA indicated a tendency for an effect of Genotype ($F_{1,23}$ = 2.77, P = 0.1), no effect of Platform position ($F_{3,69}$ = 0.37, P > 0.05) and a significant effect of the interaction between Genotype and Platform position ($F_{3,69}$ = 43.88, P < 0.001) on time spent in the target quadrant. Post hoc analyses indicated that TNR–/– mice spent more time in the target quadrant of the platform positions 2 and 3 (during the first 15 s of the first learning trials for platforms 3 and 4, respectively)

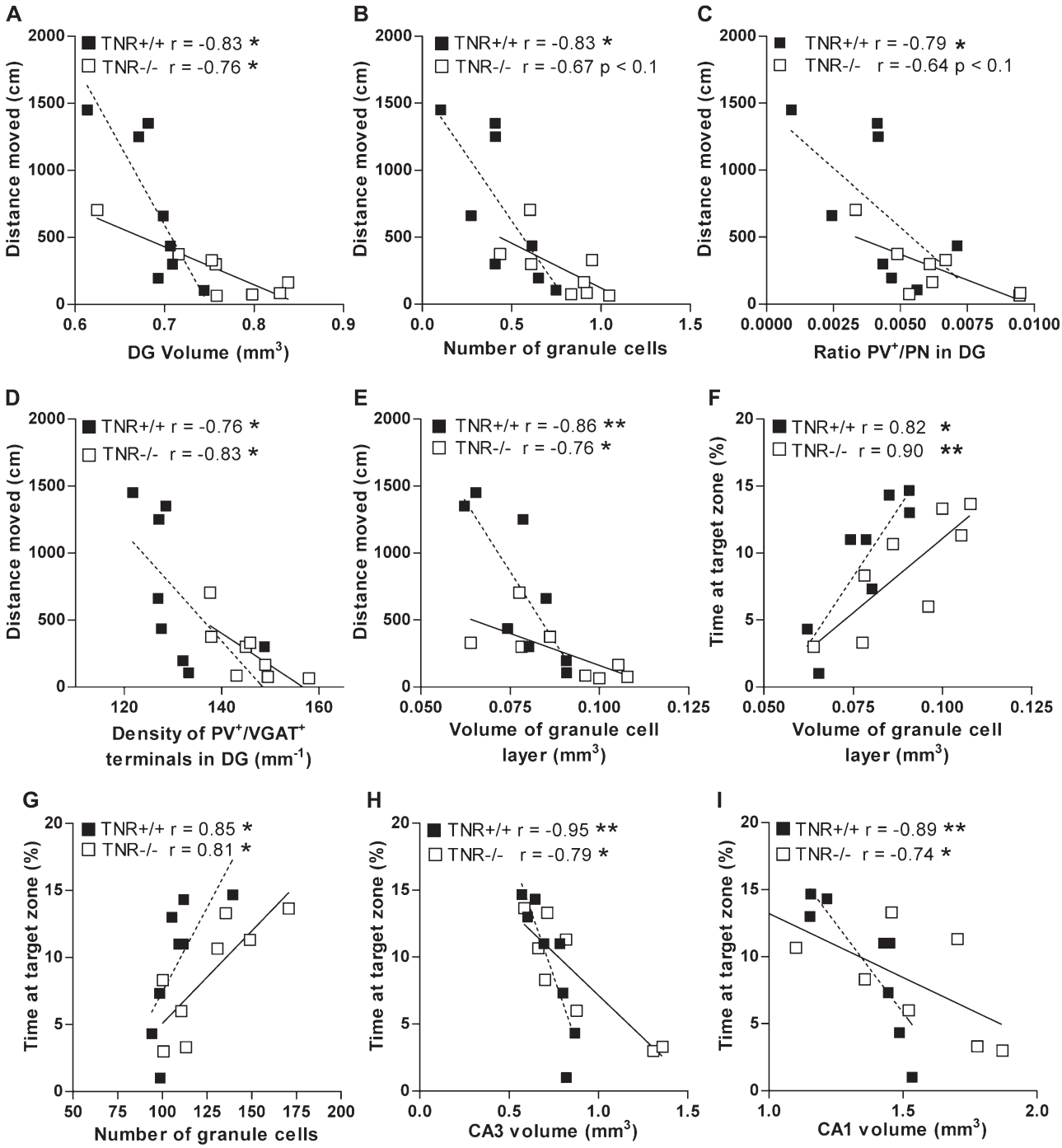

Figure 6. Significant correlations between morphology of the dentate gyrus and reversal learning in the water-maze test. Distance moved during the first trial on the second day of reversal learning (day 12) negatively correlated with volume of the dentate gyrus (*A*), number of granule cells (*B*), ratio of PV^+ to principal neurons (PNs) in the dentate gyrus (*C*), number of PV^+ and $VGAT^+$ ($PV^+/VGAT^+$) perisomatic puncta on granule cells (*D*), and volume of the granule cell layer (*E*). Time spent in the target zone during the probe trial performed at the end of learning on day 8 positively correlated with the volume of the granule cell layer (*F*) and the number of granule cells (*G*). The volume of the CA3 (*H*) and CA1 (*I*) subfields of the hippocampus negatively correlated with time spent in the target zone during the probe trial performed at the end of learning on day 8. (*A*–*I*) The Spearman correlation coefficient (*r*) and corresponding *P* value are indicated for each genotype. *,**$P < 0.05$, 0.01, respectively.

compared with TNR+/+ mice (Fig. 7*B*). These results support the interpretation of the water-maze outcome that reversal learning is enhanced in TNR–/– mice relative to TNR+/+ mice.

Test for Olfactory Learning and Reversal Learning

This test was performed to analyze whether the enhanced reversal learning of TNR–/– mice observed in the trial-to-criterion protocol of the water-maze test is restricted to spatial information. TNR–/– mice learned and reversal learned the association between an odor and a food reward better than TNR+/+ mice, indicating that TNR–/– mice show faster learning and reversal learning abilities for nonspatial information. During the first 2 pretraining trials, TNR–/– mice needed more time to enter the open field due to more time spent in risk

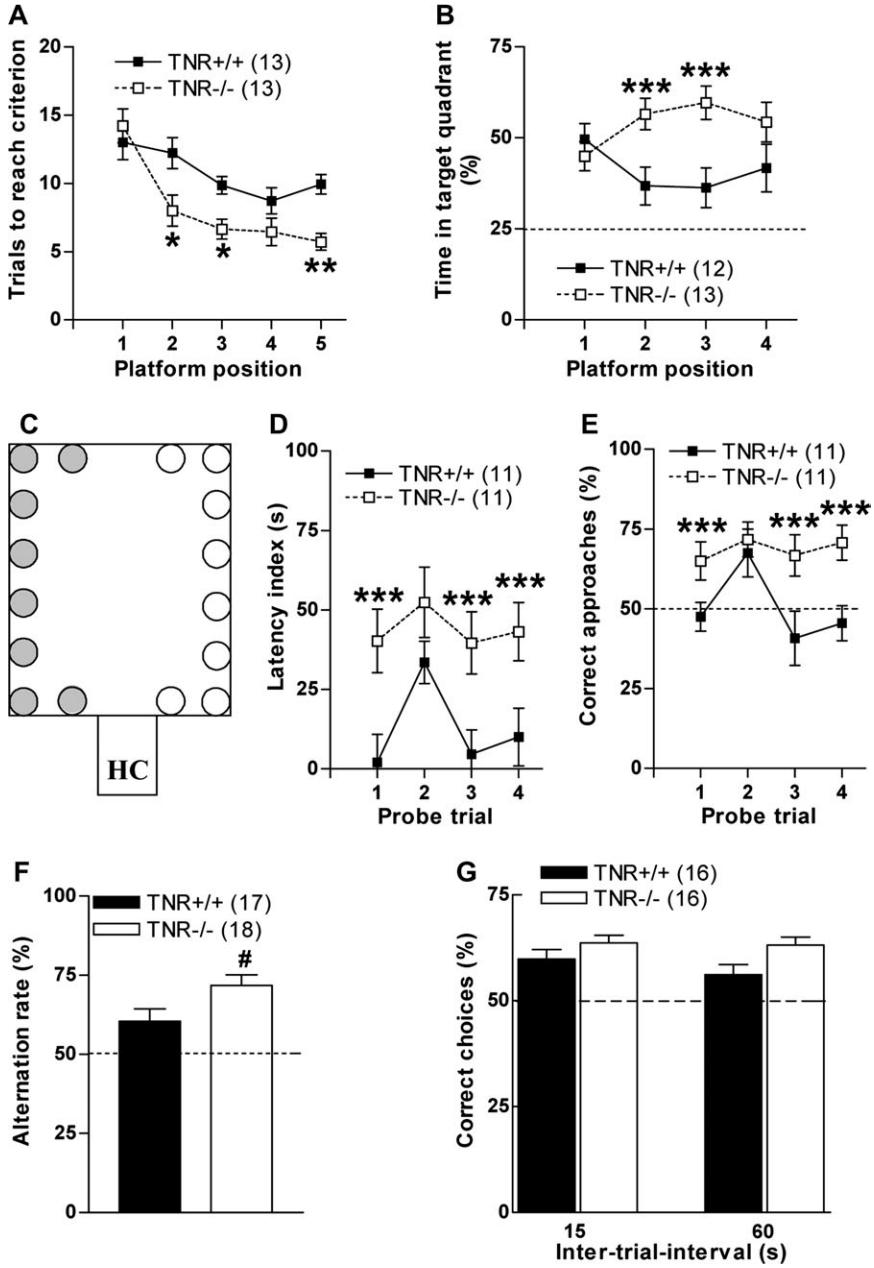

Figure 7. Enhanced reversal learning and working memory in TNR−/− mice. (*A*) TNR−/− mice needed fewer trials to reach the learning criterion (3 consecutive trials with an escape latency <15 s) compared with TNR+/+ mice for platform positions 2, 3, and 5. (*B*) The first 15-s interval of the first trials with a new platform position was used to evaluate the searching strategies for the previous platform position (e.g., the searching strategy for platform position 1 was evaluated during the first 15 s of the first trial with the platform in position 2). Both genotypes spent more time than calculated by chance (25%, indicated with a dotted line) in the correct quadrant, indicating spatial selectivity for the previously acquired platform position. TNR−/− mice spent more time in the correct quadrant for platform positions 2 and 3 compared with TNR+/+ mice. One TNR+/+ mouse found the second platform position in less than 15 s, not allowing an appropriate evaluation of the searching strategy, and was thus excluded from statistical analysis. (*C*) Scheme of the maze used for the probe trials of the olfactory learning test. The HC of a mouse was connected to an open field in which 16 dishes containing sand aromatized with either cinnamon (gray circles) or nutmeg (white circles) were placed. (*D*,*E*) Results from the probe trials of the test for olfactory learning. The probe trials 1 and 2 were performed after the first and second learning trials, respectively; the probe trials 3 and 4 were performed after the first and second reversal learning trials, respectively. In the probe trials 1, 3, and 4, TNR−/− mice approached the dishes with the correct odor faster (*D*) and more often (*E*) compared with the dishes with the incorrect odor in all probe trials and compared with TNR+/+ mice. TNR+/+ mice showed a preference for the correct odor only in probe trial 2 performed after the second learning trial, as indicated by the latency index (*D*) and percentage of correct approaches (*E*) that were higher than chance levels (0 s in *D* and 50% in *E*). (*F*,*G*) In the spontaneous alternation (*F*) and win-shift (*G*) tests, both genotypes alternated and made correct choices, respectively, more often than calculated by chance (50%, indicated with a dotted line). In the win-shift test (*D*), the enhanced frequency of correct choices of TNR−/− mice was observed using both ITIs (i.e., 15 and 60 s). The number of animals studied per group is indicated in brackets. *,**,***$P <$ 0.05, 0.01, 0.001, respectively (Newman–Keuls post hoc test after ANOVA for repeated measurements); # $P < 0.05$ (Mann–Whitney test).

assessment toward the open field compared with TNR+/+ mice (Supplementary Fig. 9). During the pretraining trial 1, but not in trials 2–4, TNR−/− mice approached the first chocolate pellet after they had entered the open field faster than TNR+/+ mice (TNR+/+ mice: 71 ± 6 s; TNR−/− mice: 51 ± 7 s; $P < 0.05$, Mann–Whitney test). No genotype-dependent differences were detected in pretraining trials 3 and 4 and during all training trials, indicating that TNR+/+ and TNR−/− had equal motivation to find and

consume the chocolate pellet (data not shown). To detect a preference for 1 of the 2 odors during the probe trials as indication of learning and memory, 2 parameters were evaluated: A latency index was calculated by subtracting the latency to approach the first dish with the correct odor from the latency to approach the first dish with the incorrect odor. Thus, a preference for the correct odor is shown by an index higher than zero, whereas indices equal to zero or lower than zero indicate no preference or a preference for the incorrect odor, respectively. As a further learning and memory parameter, the percentage of correct approaches (number of approaches to the correct dishes × 100/total number of approaches) was evaluated: Values above 50% indicate a preference for the correct odor and values of 50% or below 50% indicate no preference or a preference for the incorrect odor, respectively. When trained to associate the food reward with a determined odor, TNR−/− mice showed faster learning and better reversal learning compared with TNR+/+ mice as tested during the probe trials (Fig. 7*D*,*E*). Three-way ANOVA for repeated measures was performed using Genotype as between groups factor, and Acquisition Phase (comprising learning and reversal learning phases) and Probe Trial (first and second trials within each acquisition phase) as within group factors. Both the latency index and the percentage of correct approaches were significantly affected by Genotype (latency index: $F_{1,20}$ = 6.05; $P < 0.05$; percentage of correct approaches: $F_{1,20}$ = 9.67; $P < 0.01$) and by the interaction between Genotype, Acquisition Phase, and Probe Trial (latency index: $F_{1,20}$ = 19.72; $P < 0.001$; percentage of correct approaches: $F_{1,20}$ = 8.78; $P < 0.01$). Post hoc analyses revealed that TNR−/− mice had a higher latency index and percentage of correct approaches during the first probe trial for the learning phase and the first and second probe trials for the reversal learning phase compared with TNR+/+ mice (Fig. 7*D*,*E*). Moreover, TNR+/+ mice improved their performance from the first to the second probe trial during the learning phase but not during the reversal learning phase. The results indicate that TNR−/− mice learned the task in one trial, whereas TNR+/+ mice required 2 trials to develop a preference for the correct odor during the learning phase. Moreover, while TNR−/− mice learned a new reward-odor association after one reversal learning trial, TNR+/+ mice were not capable to learn this task after 2 trials. To test whether the performance in the olfactory test could have been affected by different levels of novelty-induced exploration or anxiety, we performed correlation analyses between the latency indices and percentages of correct approaches in the 4 probe trials and the latency to enter the open field, time in risk assessment and latency to approach the first chocolate pellet during the first pretraining trial. For both genotypes, no correlation was detected between the behavioral parameters recorded from the probe trials (indicative of the learning and reversal learning abilities) and the parameters recorded during the first pretraining trial (indicative of exploratory and anxiety-related behaviors) (Supplementary Table 2).

Spontaneous Alternation and Win-Shift Tests

The spontaneous alternation and win-shift tests were designed to characterize working memory capacities. Because no differences within groups were detected between training days 1 and 2 of the spontaneous alternation test, and between days 1 and 2 and between days 3 and 4 of the win-shift test, data were pooled for the pairs of sessions performed under the same conditions. Mice of both genotypes alternated in the spontaneous alternation test and made the correct choice in the win-shift test at a rate significantly higher than the chance level of 50% (Wilcoxon signed rank test, $P < 0.05$). In the spontaneous alternation test, TNR−/− mice alternated more frequently than TNR+/+ mice (Fig. 7*F*). Because performance in the spontaneous alternation test could be affected not only by working memory capacities, but also by exploratory strategies and anxiety, we tested the mice in a win-shift paradigm in which alternation should no more be spontaneous but functional, that is, aiming at the finding of a food reward (chocolate). Moreover, to control the levels of anxiety and motivation, the test was designed such that mice could freely move between their HC and the T-maze. With the exception of 2 TNR−/− mice and one TNR+/+ mouse, all mice were motivated to eat the chocolate in the win-shift test as indicated by the low emergence latency (the mean for all trials was 2.9 ± 0.8 s for TNR+/+ mice and 2.7 ± 0.9 s for TNR−/− mice) and by the fact that once a mouse had made a correct choice, it always ate the chocolate and no differences were detected between the genotypes (data not shown). Similarly to the spontaneous alternation test, TNR−/− mice made more correct choices compared with TNR+/+ mice regardless of the ITI used, as indicated by the significant effect of Genotype ($F_{1,30}$ = 6.12, $P < 0.05$). There was no significant effect of ITI ($F_{,30}$ = 0.33, $P > 0.05$) and of the interaction between Genotype and ITI ($F_{,30}$ = 1.22, $P > 0.05$) (Fig. 7*G*).

Step-Through Passive Avoidance and Fear Conditioning Tests

No differences were detected between genotypes in learning and memory in the step-through passive avoidance and in the fear conditioning tests, indicating that acquisition and long-term memory for fear-related information is normal in TNR−/− mice. In particular, the normal performances of TNR−/− mice in the step-through passive avoidance test and in the context version of the fear-conditioning test indicate that hippocampus-dependent function responsible for memory consolidation and retrieval of fear-related information is intact in TNR−/− mice.

In the step-through passive avoidance test, TNR−/− mice showed slightly but significantly higher latency to step-through (TNR+/+ mice: 13 ± 2 s; TNR−/− mice: 21 ± 3 s; $P < 0.05$, Mann–Whitney test) and made more stretch attend postures toward the dark compartment (TNR+/+ mice: 1.1 ± 0.8; TNR−/− mice: 3.8 ± 0.9; $P < 0.05$, Mann–Whitney test) during the conditioning trial as compared with TNR+/+ mice. During the probe trial, both genotypes enhanced the latency to step through compared with the conditioning trial and no genotype-dependent differences were detected (TNR+/+ mice: 273 ± 17 s; TNR−/− mice: 294 ± 6 s; $P > 0.05$, Mann–Whitney test). Eleven of 12 TNR−/− mice and 9 of 12 TNR+/+ mice did not step through within the maximal 300-s duration of the test.

In the fear conditioning test, both TNR+/+ and TNR−/− mice learned to associate the foot shock with the conditioned tone and context and could retrieve this information up to 1 week after conditioning as indicated by the enhanced time spent in immobility during the retrieval tests. Immediately after receiving the foot shock (Supplementary Fig. 10), mice showed fear-related behavior (immobility and tail rattling) and decreased exploratory behavior (moving and rearing). During the 24-h and

7-day retention tests, mice continued to show fear-related behaviors in response to the conditioned tone and context as indicated by the high amount of time spent in immobility (Supplementary Fig. 11). Fear-related behavior was seen also in the new cage when no tone was presented, although at lower levels than when mice were placed into the context, indicating that, despite a generalization of the context, mice could still discriminate between the context and the new cage (Supplementary Fig. 11).

New Cage and New Object Tests

The new cage and new object tests were performed to assess novelty-induced behavior. TNR–/– mice reacted more promptly to an unfamiliar environment or a new object introduced into their HC compared with TNR+/+ mice. When placed into the new cage, TNR–/– mice spent more time in a flat posture (a typical risk assessment behavior performed during the first seconds after a mouse is exposed to a new and potentially anxiogenic stimulus) (TNR+/+ mice: 3.3 ± 0.8 s; TNR–/– mice: 6.7 ± 0.6 s; $P < 0.001$, Mann–Whitney test) compared with TNR+/+ mice. No differences were detected between genotypes for number of rearings and time spent digging, climbing, and self-grooming (data not shown). After a 24-h habituation period to the new cage, both genotypes decreased the number of rearings and the time spent digging compared with the first exposure to the new cage, and increased the time spent climbing on top of the cage and eating with no differences between genotypes (data not shown). After the new object was introduced into the cage, TNR–/– mice made more stretch attend postures toward the object (TNR+/+ mice: 11 ± 1 s; TNR–/– mice: 17 ± 2 s; $P < 0.05$, Mann–Whitney test) and required less time to contact the object for the first time (TNR+/+ mice: 88 ± 14 s; TNR–/– mice: 31 ± 11 s; $P < 0.01$, Mann–Whitney test) compared with TNR+/+ mice. No differences were detected between genotypes for time spent at the object, rearing on the object, rearing in the cage, self-grooming, and immobility (data not shown).

Discussion

As a prominent feature of TNR ablation, we observed hippocampal hyperplasia associated with increased numbers of principal cells and PV^+ interneurons in all regions of the hippocampus of TNR–/– mice. To understand the mechanisms underlying this overproduction of neurons, we analyzed 7-day-old mice, an age at which TNR is expressed at high levels in the mouse hippocampus (Fuss et al. 1993). We found that cell death was reduced by almost 50% in TNR–/– mice compared with TNR+/+ littermates, whereas cell proliferation was unaffected by the mutation. Interestingly, however, only in the dentate gyrus of TNR–/– mice the ratio of inhibitory to excitatory cells was abnormally high and the perisomatic GABAergic terminals on granule cells were more numerous compared with TNR+/+ littermates. Although our findings provide evidence for a previously unrecognized developmental role of TNR, they cannot explain the region-specific effects in the dentate gyrus. To resolve this issue, further sophisticated analyses are required considering that TNR is a multifunctional molecule that may both impede and promote cell adhesion, cell migration, and neurite outgrowth (Morganti et al. 1990; Taylor et al. 1993) and influence proliferation and differentiation of neural stem–progenitor cells (Liao et al. 2008).

More intriguing than the origin of the neuronal overproduction in TNR–/– mice appeared to be the question as to how enhanced inhibitory synaptic connections affect synaptic transmission and plasticity in the dentate gyrus. We, therefore, performed electrophysiological recordings in the dentate gyrus of anesthetized mice and found a deficit in synaptic plasticity, measured as STP and LTP of field EPSPs, in TNR–/– mice. Local infusion of the $GABA_A$ receptor antagonist bicuculline restored synaptic plasticity in TNR–/– mice to the normal level observed in TNR+/+ mice, indicating that enhanced GABAergic transmission causes the impairment. This is in line with the finding of an increased ratio of PV^+ interneurons to principal cells and densities of perisomatic GABAergic synapses on principal cells specifically in the dentate gyrus of TNR–/– mice.

In addition to reduced synaptic plasticity, we found an increased LTP of population spike amplitude in pharmacologically untreated TNR–/– mice. Also, E–S potentiation, that is, an increase in population spike amplitude corrected to take into account changes in fEPSPs after induction of LTP, was larger in TNR–/– than in TNR+/+ mice. Bicuculline reduced and equalized potentiation of population spike amplitudes in TNR–/– and TNR+/+ mice. These data are consistent with the idea that increased excitability in TNR–/– mice following theta-burst stimulation in the absence, but not in the presence of bicuculline, is due to higher levels of theta-burst induced disinhibition of granule cells.

The severe impairment in STP and LTP of fEPSPs in TNR–/– mice was specific for these physiological parameters, because basal synaptic transmission and paired-pulse modulation of population spikes (almost complete suppression of spikes after second stimulation with 10- and 25-ms intervals) was not affected and paired-pulse facilitation of fEPSPs was marginally reduced in TNR–/– mice (Supplementary Material; Supplementary Fig. 3). The comparison of abnormalities in the dentate gyrus and the CA1 region of TNR–/– mice suggests that different mechanisms underlie impairments of LTP in these 2 subregions in TNR–/– mice. Although diminished inhibition in CA1 results in a homeostatic–metaplastic increase in the threshold for induction of LTP (Bukalo et al. 2007), LTP in the dentate gyrus is reduced due to elevated inhibition. In vitro recordings of LTP at mossy fiber-CA3 synapses and at associative connections between CA3 pyramidal neurons did not reveal differences between the genotypes (Supplementary Material; Supplementary Fig. 4). Consistent with this finding, our morphological analysis showed normal connectivity between PV^+ interneurons and principal cells in CA3, in contrast to CA1 and the dentate gyrus.

Another question was whether the detected structural and physiological abnormalities underpin alterations in learning and memory. As revealed by a water-maze test, learning and memory were not affected in TNR–/– mice, but reversal learning was faster than in TNR+/+ mice, as observed also in the olfactory learning test. Enhanced performance of TNR–/– mice during the reversal learning protocol of the water-maze test has been reported by Montag-Sallaz and Montag (2003) whose interpretation was that TNR–/– mice are unable to spatially locate the platform. This conclusion was based on the analysis of the swimming paths during the reversal learning trials that suggested a use of circling strategies by TNR–/– mice. The analysis of the searching strategies made by Montag-Sallaz and Montag (2003) was unfortunately biased by 2 factors: First, the duration of the trials varied between mice because it

depended on the time they needed to find, by chance, the platform at the new position. Second, the data were averaged over 2 reversal learning trials. Thus, the performance of the mice could have already been influenced by reversal learning processes or differences in motivation. In our study, we analyzed the searching strategies during the first 15 s of the first reversal learning trial, when mice are expected to search for the previously learned platform position and observed that in contrast to previous results (Montag-Sallaz and Montag 2003) TNR−/− mice are capable to spatially locate the platform. Consistently, in our trial-to-criterion protocol designed to test fast reversal learning abilities (Chen et al., 2000) TNR−/− mice not only required fewer trials to find new platform positions, but also showed high spatial selectivity for the previously learned target. Thus, their enhanced performance during reversal learning was most likely due to more efficient spatial working memory, a type of memory considered to be required for successful daily learning of a new platform location (Morris and Frey 1997; Xavier et al. 1999). To investigate this possibility, we used 2 paradigms for working memory: In both the spontaneous alternation and the win-shift tests, TNR−/− mice performed better than TNR+/+ mice. This finding is in congruence with faster reversal learning and strongly supports the idea that working memory of TNR−/− mice is more efficient than in TNR+/+ mice. In agreement with the idea that TNR ablation improved reversal learning and working memory but not general hippocampal-dependent learning and memory, TNR−/− did not differ form the TNR+/+ mice in the contextual fear conditioning and step-through passive avoidance tests.

TNR−/− mice showed enhanced risk assessment when exposed to a new environment, as observed in the new cage and new object test and in the conditioning trial of the step-through passive avoidance test. Enhanced risk assessment also explains the higher emergence latency and latency to eat the chocolate shown by TNR−/− mice during the first 2 pretraining sessions preceding the test for olfactory learning. Interestingly, despite the elevated time spent in risk assessment, TNR−/− mice were faster than TNR+/+ in approaching a new stimulus as observed in the new object test and during pretraining for the test for olfactory learning when the latency to approach the chocolate pellet was lower for TNR−/− than for TNR+/+ mice. Taken together, these results suggest that TNR deficiency enhances the attention to new stimuli, increasing the risk assessment and reactivity to investigate them. It could be argued that the enhanced performance of TNR−/− mice in the tests for learning and memory was due to their enhanced reactivity to new stimuli. We tend to exclude this hypothesis for several reasons. First, with the exception of the first minutes of the tests, all other parameters for general novelty-induced exploratory behavior and anxiety did not differ between genotypes in the new cage and new object tests. Second, no differences in the latency to start and conclude a trial were detected between genotypes during the training trails of the win-shift and olfactory learning tests. Third, in the olfactory learning test, no correlation was found between novelty-induced behavior during pretraining and learning and memory abilities. Finally, we could not detect any correlation between the performance in the water-maze and the new object tests.

To study which structural parameters of the CA1, CA3, and dentate gyrus are related to cognitive abilities, we performed correlation analyses of morphological and behavioral data. We found that, even within one genotype, faster reversal learning correlated with a higher number of granule cells, ratios of PV^+ interneurons to granule cells and densities of PV^+ terminals on granule cell bodies in the dentate gyrus. This suggests that the number of PV^+ interneurons and granule cells, the ratio between them, and the density of perisomatic PV^+ synapses in the dentate gyrus affect the individual rate of reversal learning. These results are in agreement with the view that the dentate gyrus is important for fast integration of new spatial information, indicating that enhanced perisomatic inhibition in the dentate gyrus facilitates this cognitive function. In support of this notion is a recent observation that reduction of excitatory drive by conditional ablation of the GluR-A and GluR-D subunits of α-amino-3-hydroxyl-5-methyl-4-isoxazole-propionate (AMPA) receptors in PV^+ interneurons impairs specifically working and episodic-like memories (Fuchs et al. 2007). Similarly, administration of the psychotomimetic phencyclidine reduces the density of PV^+ interneurons in the dentate gyrus and impairs reversal learning in rats (Abdul-Monim et al. 2007). Conversely, C57BL/6J mice experiencing maternal separation have a decreased number of neurons in the dentate gyrus and slower reversal-learning rate in the Barnes maze, whereas learning and memory were unaffected compared with control mice reared under normal conditions (Fabricius et al. 2008). Furthermore, several lines of evidence indicate that the dentate gyrus is crucial for spatial reversal learning and working memory but not for consolidation and retrieval of reference memory (Jung and McNaughton 1993; Xavier et al. 1999; Neill et al. 2001; Lee and Kesner 2004; Rolls and Kesner 2006; Hernandez-Rabaza et al. 2007; Niewoehner et al. 2007). For instance, it was recently shown that granule cells in the dentate gyrus play an important role in rapid formation of a new contextual memory and discriminating it from previously encountered similar contexts (McHugh et al. 2007). This cognitive process is defined as pattern separation and can be supportive of reversal learning as tested in the present study.

With a view on the physiological mechanisms underlying this remarkable phenotype, we suggest that enhanced inhibition in the dentate gyrus may allow for a better signal-to-noise ratio for information impinging onto the granule cells from the entorhinal cortex. Indeed, the dentate gyrus is, within the hippocampus, the primary target of the majority of entorhinal afferents that terminate in a laminar-specific fashion on granule cell dendrites and carry sensory information on multiple modalities about the external world. It has thus been suggested that the dentate gyrus serves as a gate, filtering excitation from the entorhinal cortex (Hsu 2007), a function that may explain the conspicuous extensive inhibitory network of cells that are involved in synchronizing the rhythmic firing of the granule cells (Ribak and Shapiro 2007). In this context, enhanced inhibition would be functional by allowing the processing of only new relevant information thereby improving working memory and reversal learning. An increase in signal-to-noise ratio may be achieved by suppression of background firing of neurons and/or, as suggested by our analysis of population spike LTP and E-S potentiation, by an increase in the activity-dependent disinhibition of neurons encoding task-relevant features of the environment. This region-specific facilitation of activity-dependent changes in excitability may improve filtering of sensory information and facilitate faster reversal learning. A region-specific function of LTP has been

reported by Okada et al. (2003) who showed that regional enhancement of LTP via expression of Ca^{2+}-permeable AMPA receptors caused opposite behavioral consequences on the water-maze task: Rats with enhanced CA1 LTP showed shorter escape latency and better probe test performance, whereas those with enhanced dentate gyrus LTP showed impaired performance. It is noteworthy that both working memory and reversal learning require not only that the newest relevant information is consolidated into a new memory trace but also that previously learned memories do not interfere with acquisition and consolidation of new memories. Thus, the reduced STP and LTP of fEPSPs in TNR−/− dentate gyrus may minimize this interference in the dentate gyrus and thereby enhance working memory and reversal learning.

In conclusion, our findings indicate that TNR ablation reduces cell death during early postnatal development leading to an increased number of neurons in the adult hippocampus. An enhancement of the ratio of PV^+ interneurons to granule cells and the ensuring increase in the perisomatic PV^+ GABAergic connections to granule cells cause a reduction in LTP of synaptic responses and enhanced population spike LTP in the dentate gyrus, highlighting the importance of PV+ interneuron population in determining the physiological properties of granule cells. Furthermore, the increased perisomatic GABAergic terminals on granule cells of TNR−/− mice correspond to faster reversal learning and enhanced working memory abilities of these mice. The observation that within TNR+/+ mice interindividual variability in the structure of the dentate gyrus predicts the rate of reversal learning confirms our interpretation of the described functional alterations of TNR−/− mice and highlights the importance of perisomatic inhibition in regulating dentate gyrus control on specific cognitive functions.

Supplementary Material

Supplementary material can be found at: http://www.cercor.oxfordjournals.org/.

Funding

DAAD fellowship to L.S. and grants from the Deutsche Forschungsgemeinschaft (Di 702/4-1,2,3 to A.D.; SFB 470 and SPP 1172 to M.S.).

Notes

We thank Emanuela Szpotowicz for technical assistance and Achim Dahlmann for genotyping of mice. M.S. is New Jersey Professor of Spinal Cord Research. *Conflict of Interest*: None declared.

References

Abdul-Monim Z, Neill JC, Reynolds GP. 2007. Sub-chronic psychotomimetic phencyclidine induces deficits in reversal learning and alterations in parvalbumin-immunoreactive expression in the rat. J Psychopharmacol. 21:198–205.

Bampton ET, Gray RA, Large CH. 1999. Electrophysiological characterisation of the dentate gyrus in five inbred strains of mouse. Brain Res. 841:123–134.

Barnard EA, Skolnick P, Olsen RW, Mohler H, Diehard W, Baggie G, Bastrop C, Bateson AN, Langer SZ. 1998. International union of pharmacology. XV. Subtypes of gamma-aminobutyric acidA receptors: classification on the basis of subunit structure and receptor function. Pharmacol Rev. 50:291–313.

Berghuis P, Dobszay MB, Sousa KM, Schulte G, Mager PP, Härtig W, Görcs TJ, Zilberter Y, Ernfors P, Harkany T. 2004. Brain-derived neurotrophic factor controls functional differentiation and microcircuit formation of selectively isolated fast-spiking GABAergic interneurons. Eur J Neurosci. 20:1290–1306.

Brandewiede J, Schachner M, Morellini F. 2005. Ethological analysis of the senescence-accelerated P/8 mouse. Behav Brain Res. 158:109–121.

Bukalo O, Schachner M, Dityatev A. 2007. Hippocampal metaplasticity induced by deficiency in the extracellular matrix glycoprotein tenascin-R. J Neurosci. 27:6019–6028.

Chen G, Chen KS, Knox J, Inglis J, Bernard A, Martin SJ, Justice A, McConlogue L, Games D, Freedman SB, et al. 2000. A learning deficit related to age and beta-amyloid plaques in a mouse model of Alzheimer's disease. Nature. 408:975–979.

Cobb SR, Buhl EH, Halasy K, Paulsen O, Somogyi P. 1995. Synchronization of neuronal activity in hippocampus by individual GABAergic interneurons. Nature. 378:75–78.

Davis S, Bliss TV, Dutrieux G, Laroche S, Errington ML. 1997. Induction and duration of long-term potentiation in the hippocampus of the freely moving mouse. J Neurosci Methods. 75:75–80.

Errington ML, Bliss TV, Morris RJ, Laroche S, Davis S. 1997. Long-term potentiation in awake mutant mice. Nature. 387:666–667.

Fabricius K, Wörtwein G, Pakkenberg B. 2008. The impact of maternal separation on adult mouse behavior and on the total neuron number in the mouse hippocampus. Brain Struct Funct. 212:403–416.

Fellini L, Schachner M, Morellini F. 2006. Adult but not aged C57BL/6 male mice are capable of using geometry for orientation. Learn Mem. 13:473–481.

Freitag S, Schachner M, Morellini F. 2003. Behavioral alterations in mice deficient for the extracellular matrix glycoprotein tenascin-R. Behav Brain Res. 145:189–207.

Freund TF. 2003. Interneuron diversity series: rhythm and mood in perisomatic inhibition. Trends Neurosci. 26:489–495.

Freund TF, Buzsáki G. 1996. Interneurons of the hippocampus. Hippocampus. 6:347–470.

Fuchs EC, Zivkovic AR, Cunningham MO, Middleton S, Lebeau FE, Bannerman DM, Rozov A, Whittington MA, Traub RD, Rawlins JN, et al. 2007. Recruitment of parvalbumin-positive interneurons determines hippocampal function and associated behavior. Neuron. 53:591–604.

Fuss B, Wintergerst ES, Bartsch U, Schachner M. 1993. Molecular characterization and in situ mRNA localization of the neural recognition molecule J1-160/180: a modular structure similar to tenascin. J Cell Biol. 120:1237–1249.

Hanse E, Gustafsson B. 1992. Long-term potentiation and field EPSPs in the lateral and medial perforant paths in the dentate gyrus in vitro: a comparison. Eur J Neurosci. 4:1191–1201.

Härtig W, Brauer K, Brückner G. 1992. *Wisteria floribunda* agglutinin-labelled nets surround parvalbumin-containing neurons. Neuroreport. 3:869–872.

Hernandez-Rabaza V, Barcia JA, Llorens-Martin M, Trejo JL, Canales JJ. 2007. Spared place and object-place learning but limited spatial working memory capacity in rats with selective lesions of the dentate gyrus. Brain Res Bull. 72:315–323.

Hsu D. 2007. The dentate gyrus as a filter or gate: a look back and a look ahead. Prog Brain Res. 163:601–613.

Irintchev A, Rollenhagen A, Troncoso E, Kiss JZ, Schachner M. 2005. Structural and functional aberrations in the cerebral cortex of tenascin-C deficient mice. Cereb Cortex. 15:950–962.

Jung MW, McNaughton BL. 1993. Spatial selectivity of unit activity in the hippocampal granular layer. Hippocampus. 3:165–182.

Lee I, Kesner RP. 2004. Encoding versus retrieval of spatial memory: double dissociation between the dentate gyrus and the perforant path inputs into CA3 in the dorsal hippocampus. Hippocampus. 14:66–76.

Lewis DA, Hashimoto T, Volk DW. 2005. Cortical inhibitory neurons and schizophrenia. Nat Rev Neurosci. 6:312–324.

Liao H, Huang W, Schachner M, Guan Y, Guo J, Yan J, Qin J, Bai X, Zhang L. 2008. Beta 1 integrin mediated effects of tenascin-R domains EGFL and FN6-8 on neural stem/progenitor cell proliferation and differentiation in vitro. J Biol Chem. 283:27927–27936.

Long JM, Kalehua AN, Muth NJ, Hengemihle JM, Jucker M, Calhoun ME, Ingram DK, Mouton PR. 1998. Stereological estimation of total microglia number in mouse hippocampus. J Neurosci Methods. 84:101–108.
Madden SD, Donovan M, Cotter TG. 2007. Key apoptosis regulating proteins are down-regulated during postnatal tissue development. Int J Dev Biol. 51:415–423.
McBain CJ, Fisahn A. 2001. Interneurons unbound. Nat Rev Neurosci. 2:11–23.
McHugh TJ, Jones MW, Quinn JJ, Balthasarm N, Coppari R, Elmquist JK, Lowell BB, Fanselow MS, Wilson MA, Tonegawa S. 2007. Dentate gyrus NMDA receptors mediate rapid pattern separation in the hippocampal network. Science. 317:94–99.
Mitchell SJ, Silver RA. 2003. Shunting inhibition modulates neuronal gain during synaptic excitation. Neuron. 38:433–445.
Montag-Sallaz M, Montag D. 2003. Severe cognitive and motor coordination deficits in tenascin-R-deficient mice. Genes Brain Behav. 2:20–31.
Morellini F, Schachner M. 2006. Enhanced novelty-induced activity, reduced anxiety, delayed resynchronization to daylight reversal and weaker muscle strength in tenascin-C-deficient mice. Eur J Neurosci. 23:1255–1268.
Morganti MC, Taylor J, Pesheva P, Schachner M. 1990. Oligodendrocyte-derived J1-160/180 extracellular matrix glycoproteins are adhesive or repulsive depending on the partner cell type and time of interaction. Exp Neurol. 109:98–110.
Morris RG, Frey U. 1997. Hippocampal synaptic plasticity: role in spatial learning or the automatic recording of attended experience? Philos Trans R Soc Lond B Biol Sci. 352:1489–1503.
Neill JC, Sarkisian MR, Wang Y, Liu Z, Yu L, Tandon P, Zhang G, Holmes GL, Geller AI. 2001. Enhanced auditory reversal learning by genetic activation of protein kinase C in small groups of rat hippocampal neurons. Brain Res Mol Brain Res. 93:127–136.
Niewoehner B, Single FN, Hvalby O, Jensen V, Borgloh SM, Seeburg PH, Rawlins JN, Sprengel R, Bannerman DM. 2007. Impaired spatial working memory but spared spatial reference memory following functional loss of NMDA receptors in the dentate gyrus. Eur J Neurosci. 25:837–846.
Nikonenko A, Schmidt S, Skibo G, Brückner G, Schachner M. 2003. Tenascin-R-deficient mice show structural alterations of symmetric perisomatic synapses in the CA1 region of the hippocampus. J Comp Neurol. 456:338–349.
Nikonenko AG, Sun M, Lepsveridze E, Apostolova I, Petrova I, Irintchev A, Dityatev A, Schachner M. 2006. Enhanced perisomatic inhibition and impaired long-term potentiation in the CA1 region of juvenile CHL1-deficient mice. Eur J Neurosci. 23:1839–1852.
Nosten-Bertrand M, Errington ML, Murphy KP, Tokugawa Y, Barboni E, Kozlova E, Michalovich D, Morris RG, Silver J, Stewart CL, et al. 1996. Normal spatial learning despite regional inhibition of LTP in mice lacking Thy-1. Nature. 379:826–829.
Okada T, Yamada N, Tsuzuki K, Horikawa HP, Tanaka K, Ozawa S. 2003. Long-term potentiation in the hippocampal CA1 area and dentate gyrus plays different roles in spatial learning. Eur J Neurosci. 17:341–349.
Reznikov KY. 1991. Cell proliferation and cytogenesis in the mouse hippocampus. Adv Anat Embryol Cell Biol. 122:1–74.
Ribak CE, Shapiro LA. 2007. Ultrastructure and synaptic connectivity of cell types in the adult rat dentate gyrus. Prog Brain Res. 163:155–166.
Rolls ET, Kesner RP. 2006. A computational theory of hippocampal function, and empirical tests of the theory. Prog Neurobiol. 79:1–48.
Snyder JS, Kee N, Wojtowicz JM. 2001. Effects of adult neurogenesis on synaptic plasticity in the rat dentate gyrus. J Neurophysiol. 85:2423–2431.
Stoenica L, Senkov O, Gerardy-Schahn R, Weinhold B, Schachner M, Dityatev A. 2006. In vivo synaptic plasticity in the dentate gyrus of mice deficient in the neural cell adhesion molecule NCAM or its polysialic acid. Eur J Neurosci. 23:2255–2264.
Taylor J, Pesheva P, Schachner M. 1993. Influence of janusin and tenascin on growth cone behavior in vitro. J Neurosci Res. 35:347–362.
Weber P, Bartsch U, Rasband MN, Czaniera R, Lang Y, Bluethmann H, Margolis RU, Levinson SR, Shrager P, Montag D, et al. 1999. Mice deficient for tenascin-R display alterations of the extracellular matrix and decreased axonal conduction velocities in the CNS. J Neurosci. 19:4245–4262.
Wei W, Zhang N, Peng Z, Houser CR, Mody I. 2003. Perisynaptic localization of delta subunit-containing GABAA receptors and their activation by GABA spillover in the mouse dentate gyrus. J Neurosci. 23:10650–10661.
Wintergerst ES, Fuss B, Bartsch U. 1993. Localization of janusin mRNA in the central nervous system of the developing and adult mouse. Eur J Neurosci. 5:299–310.
Woo NH, Lu B. 2006. Regulation of cortical interneurons by neurotrophins: from development to cognitive disorders. Neuroscientist. 12:43–56.
Wood ER, Dudchenko PA, Robitsek RJ, Eichenbaum H. 2000. Hippocampal neurons encode information about different types of memory episodes occurring in the same location. Neuron. 27:623–633.
Woodworth A, Fiete D, Baenziger JU. 2002. Spatial and temporal regulation of tenascin-R glycosylation in the cerebellum. J Biol Chem. 277:50941–50947.
Xavier GF, Oliveira-Filho FJ, Santos AM. 1999. Dentate gyrus-selective colchicine lesion and disruption of performance in spatial tasks: difficulties in "place strategy" because of a lack of flexibility in the use of environmental cues? Hippocampus. 9: 668–681.